MASTER THESIS

Development of an origami based, magnetically actuated, endovascular locomotion device

Greenlight-version (05-02-2025)

JOANNES CORNELIUS SCHAGEN

FACULTY OF ENGINEERING TECHNOLOGY

DEPARTMENT OF BIOMECHANICAL ENGINEERING

EXAMINATION COMMITTEE

PROF. DR. S MISRA
DR. V. KALPATHY VENKITESWARAN
IR. E.E.G. HEKMAN

DOCUMENT NUMBER

FEBRUARY 5, 2025

Thesis submitted by
Joannes Cornelius Schagen
under the supervision of
prof. dr. S. Misra,
dr. V. Kalpathy Venkiteswaran, and
ir. E.E.G. Hekman
in order to fulfil the necessary requirements to obtain a Master's degree in
Biomechanical Engineering at the University of Twente
and defended on
Friday, 7th of March, 2025

SURGICAL ROBOTICS
LABORATORY

WWW.SURGICALROBOTICSLAB.NL

Abstract

Despite the benefits of Minimally Invasive Surgery over open surgery, there are still difficulties hard to overcome. These difficulties lie for a large part in the learning curve that is required to operate the surgical tools necessary for MIS. It is thus not supring that easier methods of MIS are being developed, such as capsule robots that navigate through the human body by using the peristaltic movement of the diegestive tract or magnetic actuation. Applying this technology to the arteries however, is more difficult. The smaller scale and vulnerability of the artery wall requires for an alternative design. The aim of this thesis is to develop an origami based and magnetically actuated device that could assist endovascular MIS. To set limits on the design solutions, it was chosen to focus on one specific MIS. This MIS is the endovascular repair (EVAR) of Abdominal Aortic Anuerysms (AAA). Using EVAR as case study helped creating requirements and gave insight in the current struggles of MIS. Background research was done to gain further insight in, amongst others, AAA, origami engineering, living hinges, and the current state-of-the-art. The knowledge gained from the background research aided in the development of the requirements as well. Based on these requirements three concepts were developed, which after evaluation resulted in one final concept, using three modules to move through an artery like a piston. The concept was then further defined and additional requirements were set up for each module. Based on the requirements the waterbomb tesselation and the collapsable tower were integrated into the final design. A prototype was developed and tested on its core abilities. The prototype provides promosing evidence to be a valid proof of principle. However, due to scale and the use of specific materials the design is not yet realistic. The thesis will end with recommandations for future development and the conclusion.

Table of Contents

Abstract **i**

Table of Contents **ii**

List of Figures **iv**

List of Tables **v**

1 Introduction **1**

2 Literature research **2**
2.1 Design process . . . 2
2.2 Origami engineering . . . 2
2.3 Origami tesselations . . . 3
2.4 Living hinges . . . 4
2.5 Magnetic actuation . . . 5
2.6 AAA . . . 6
2.7 State of the art . . . 6
2.8 Mass-spring-damper model . . . 7
2.9 Additive Manufacturing . . . 8

3 Preliminary Design **9**
3.1 Requirements . . . 9
3.2 Ideation . . . 10
3.3 Concepts . . . 10
3.3.1 Self-propelled vine robot . . . 10
3.3.2 Popping screwthread . . . 12
3.3.3 Negative-poison ratio worm . . . 12
3.4 Choosing a concept to continue . . . 13

4 Final design **13**
4.1 Locomotion . . . 13
4.1.1 Control . . . 14
4.1.2 Sequences . . . 15
4.2 Additional Requirements . . . 17
4.2.1 Requirements for RM . . . 17
4.2.2 Requirements for AXM . . . 18
4.3 Origami patterns . . . 19
4.3.1 Origami pattern for RM . . . 19
4.3.2 Origami pattern for AXM . . . 20
4.4 Material . . . 23
4.5 Magnet placement . . . 27
4.5.1 Magnet placement for RM-module . . . 27
4.5.2 Magnet placement for AXM-module . . . 29
4.5.3 Improvements . . . 30

5 Prototype experiments **31**
5.1 Setup . . . 31
5.2 Slow wave input . . . 32
5.3 Puls input . . . 33
5.4 Integration test . . . 34
5.5 Discussion . . . 35

6 Mass-spring-damper model **36**
6.1 Creating the model . . . 36
6.2 Finding the correct parameters . . . 37
6.3 Using the model to find prototype improvements . . . 38
6.3.1 RM expansionrate . . . 38
6.3.2 AXM speed . . . 38
6.4 Shortcomings of the model . . . 39
6.5 Conclusion . . . 39

7 Evaluation and discussion **40**
7.1 Requirements met . . . 40
7.2 Requirements not met . . . 41
7.3 Requirements that need to be tested . . . 41
7.4 Potential uses . . . 42

8 Conclusion **42**

References **43**

9 Appendex **47**
9.1 Morphological diagram . . . 47
9.2 Lasercutter setup . . . 48
9.3 Lasercutter results . . . 49
9.3.1 Results 50g paper . . . 49
9.3.2 Results 80g paper . . . 50
9.3.3 Result table . . . 51

List of Figures

1 a and b: pictures of origami crane flapping its wings [6]. c: crease pattern of an origami crane, with mountain and valley folds [7] . . . 3
2 Picture showing how origami engineering is used in satalites and how their crease pattern can be recreated with paper. . . . 3
3 Tesselation patterns of interest for this thesis (a)Waterbomb, (b)Lang Oval Tesselation, (c)Hoffman waterbomb, (d)Hoffman star-triangles,(e)Resch triangle tesselation. [9] . . . 4
4 Living hinges as used in the Robotime electric guitar [10] . . . 5
5 Diagram showing the forces created by the bipolar magnet inside a uniform magnetic field resulting in the rotation of the magnet. . . . 5
6 Venn Diagram visualising the current state of the art of magnetically actuated, origami-based, endovascular devices. A: Magnetically actuated, origami-inspired endoscope capsule. B: Origami-based ICMRI cathether. C: Compliant magnetic capsule robot to traverse the aorta. [27] [55] [57] . . . 7
7 Sketch of a 1 DOF Mass-Spring-Damper Model . . . 7
8 Step-by-step visualisation of the working of the koleidocycle, starting with a, then b, until e. After e the cycle starts again with a. [23] . . . 11
9 Sketch of the self-propelled vine robot pulling a stent . . . 11
10 Sketch of the popping screwthread concept . . . 12
11 Early concept sketch of the Negative-poison ratio worm, consisting of 6 identical modules. . . 13
12 Sketch of the final concept, consisting of the three modules: RM1, AXM, and RM2 . . . 14
13 Sketch of predicted movement during amplitude-sequence method . . . 15
14 Visualisation of code used in locomotion diagram with two examples. (a) RM1 expanded, AXM and RM2 collapsed. (b)RM1 partially expanded, AXM and RM2 expanded . . . 15
15 Explored locomotion sequences. (a) Ideal sequence.(b)First 1 DOF sequence (c)2 DOF sequence (d)Second 1 DOF sequence . . . 17
16 Visualisation to show that standard origami creases result in collisions (red), and how creating a channel (green) can prevent this . . . 20
17 Picture of the first AXM design . . . 20
18 Picture of the Miuri tube. . . . 21
19 Picture of a 5x2 ring with the Huffman star-triangle tesselation. . . . 22
20 Picture of Huffman star-triangle tube, tesselation is 4x10 . . . 22
21 Picture of a 7 layered collapsable tower dodecagon . . . 23
22 Picture of the "Collapsable Tower Dodecagon V2 With Sectioned Folds" without sectioned folds. . . . 23
23 3D printed prototypes of the waterbomb tesselation using living hinges . . . 24
24 Mould, ejector, and prototype made during this thesis . . . 25
25 Unfolded waterbomb prototype, made by using clear packaging tape and PLA panels. . . . 26
26 Assembly of an RM prototype, using a stencil to place the panels at the desired location . . . 27
27 Magnet placement and its resulting simulated behaviour . . . 29
28 Sketch of setup used during the waterbomb experiment . . . 31
29 Results of the slow changing field experiment for both the AXM and RM module . . . 32
30 Frames of AXM module being both collapsed and exanded during the slow wave input experiment. Green: Baseline, Blue:maximum retraction,Red:maximum expansion . . . 33
31 Frames of RM module being both collapsed and exanded during the slow wave input experiment. Green: Baseline, Blue:maximum retraction,Red:maximum expansion . . . 33
32 Average normalised expansion rate over four cycles for (a): the RM. And (b) the AXM . . . 34
33 Altered MSD model used in this thesis for simulating the indidivual behaviour of the modules 36
34 Graph visualising difference between model and reality. Blue: Simulation. Black-dashed: Max and Min values of prototype during experiment. . . . 38

List of Tables

1 Design Requirements for origami magnetic capsule robot 9
2 Additional Requirements for origami magnetic capsule robot 18
3 Retraction index of the different magnet placement configurations for the RM module 29
4 Settling times of RM and AXM. 34
5 Parameters used in the MSD model and its real life counterparts 37
6 Parameter values used in simulation 37
7 Evaluation of all requirements based on final prototype 40
8 Results 50 gsm paper. C=cut, C/G=Almost good engraving but parts are cut, G=good engraving, G/N=There is engraving but it is very shallow, N=no engraving, P=perforation . 51
9 Results 80 gsm paper. C=cut, C/G=Almost good engraving but parts are cut, G=good engraving, G/N=There is engraving but it is very shallow, N=no engraving, P=perforation . 51

1 Introduction

With origami a complex 3-dimensional object can be created from a simple piece of paper, without tearing or glueing. This ancient art form can now also be seen in many engineering projects, as device capable of completely changing its shape without any glueing, welding, or cutting can be very useful. For example in satellites. These need to be compact when launched, but as big as possible when in orbit. On a smaller scale in airbags, that are folded using origami patterns to ensure rapid expansion in the right shape. Going even smaller, origami based tools are also being developed and used in the healthcare industry. Especially Minimally Invasive Surgery (MIS) benefits from this technology. This surgical discipline aims to perform surgical procedures without making any large incisions. MIS is only possible since the 1980s and was only initially possible due to the development of the rod lens systems, the reduction in size of video cameras, and specialised surgical tools [25] [33]. But in the last few decades cameras have become even smaller, allowing for the development of observative capsule robots for inside the digestive tract or even microscopic cameras on a string able to traverse the arteries [19] [41]. These capsule robots are, however, unable to perform any surgical activities and rely on the peristaltic movement of the digestive tract to move the device forward. Some of the devices are able to move by deforming their body, making it possible to aim the camera at a desired location [52]. Such robots that have an elastic body which can be deformed in order to perform actions, are called soft-robots [59].

Origami is a very promosing technologi for the development of MIS surgical tools. Having a tool that can alter its shape to be more compact during placement, yet be open and functional inside the human body, can be very convenient. Making it possible to actuate these tools via a remote magnetically field provides more freedom of movement and makes surgery even less invasive. Soft robots for MIS are already in development but are either not endovascular, not magnetically actuated, or do not apply origami engineering [27] [55]. Thus this master thesis aims to develop a device that can do all three, be origami-based, magnetically actuated, and useful for endovascular MIS. The endovascular MIS that was chosen as the target for the design of the device was the treatment of Abdominal Aortic Aneurysm (AAA) via Endovascular Repair (EVAR). EVAR is the alternative to open surgical AAA repair and although more safe is also difficult and requires high precision of the surgeons [28]. Developing a tool that compactly can be inserted inside the aorta and move towards the difficult-to-reach spots could make EVAR less difficult and take less time.

The aim of this master thesis is to develop a soft robot that can locomote through endovascular systems via magnetic actuation using origami engineering. In section 2 an overview is given of the the design process used, but going especially indepth on the background of origami, the workings of magnetic actuation, and the current state-of-the-art. The section ends with a quick introduction in Mass-Spring-Damper (MSD) models and Additive Manufacturing (AM). Section 3 set the boundaries for the design by defining the initial requirements. Within these boundaries 3 concepts are created, all with a different type of locomotion. The section ends explaining that all 3 concepts have flaws, defining a fourth final concept. In section 4 this final concept is further defined going more indepth on the method of locomotion and the additional requirements that were set to make this locomotion possible. Following these requirements different origami patterns, materials, production methods, and magnet placements were explored and selected to define the final design and make it possible to create a prototype. Section 5 describes the three tests done with the prototype. The first test uses a slow rising magnetic field as input to determine the maximum expansion rate and gain insight in the folding behaviour of the modules. The second test uses a field that every second instantly switches from direction, this experiment is done to determine the expansion speed and gain a data for the model created in next section. the last experiment is an integration test of all three the modules inside a tube, as a final test. The results are also discussed in this chapter, followed by a quick discussion. In section 6 a model is proposed to simulate the expanding behaviour of the individual modules. After finding the correct parameters to fit inside the altered MSD model, the behaviour of the module during the second experiment can be simulated. the model also is used to simulate desired behaviour in order to find out what adjustments need to be made on the prototype to make it fulfil the requirement RMexpansion rate and AXM speed. In chapter 7 the final design and the results of the experiment are measured against the requirements. Going more indepth in the reason how each requirement was met, why it some requirements were not met, and which requirements still need further research. This section will also dive into the potential use cases for this device. The thesis ends with the conclusion in section 8, summarising the process, the findings, and the flaws of this thesis.

2 Literature research

This chapter contains the background research that formed the base on which the locomotive device was created. There is a lot of research already (being) done on the subject of origami engineering, as well as medical research on the improvement and facilitation of minimally invasive surgeries. Diving into both topics, as well as finding the right design method and looking into the current state of the art, eventually led to a series of requirements which formed the base for the ideation phase. Modeling and additive manufacturing are also discussed as these topics allow the requirements to be evaluated.

2.1 Design process

The design process can be approached in different ways. Corinne Kruger identified four design strategies: Problem driven, Solution driven, Information driven, and Knowledge driven [37]. The most commonly used is the problem-driven design. This method requires the designer to understand the design problem and create a solution around it. Using this approach leads to many requirements being identified and high-quality solutions, however, these solutions are not very creative. A solution-driven design process can be used instead to enhance creativity. The design problem in solution-driven design is poorly defined, only defining when that is needed. This leads to a much larger search space and more varied solutions. The evaluation of these solutions focuses on (re)defining the problem.

This thesis aims to find a novel transporter design using origami and magnetic actuation for MIS. The application of treating an aortic aneurysm is more a guideline than a hard-defined problem and creativity is of utmost importance. Thus instead of hard-defining the requirements to fit an Aortic Aneurysm and following the problem-driven design process. A solution-driven design process will be used.

Problem-driven design and solution-driven design have parallels with the distinction between market-driven and technology-driven innovation in management [30] [17]. Market-driven innovation is innovating based on what customers want, a tool for aortic aneurysms in this case. Technology-driven innovation is when the technology is developed first, where after an application for that is found. In this case, this would be a push to develop a small origami-magnetic actuated locomotion device for inside the human body.

2.2 Origami engineering

The technology that will drive the innovation is the use of magnets to control the folds of origami patterns. Origami is the art of folding paper into a 3d structure. It has existed for hundreds if not thousands of years, with the first books on recreational origami made in the 1800s but experts believe the art to be much older than that [21] [8].

At the foundation of origami lies the crease pattern, this pattern instructs how to fold the paper to construct the desired shape. One of the best-known origami patterns is the paper aeroplane. Undoing the folds of the aeroplane to transform it back into a piece of paper creates a piece of paper with folding lines, this is a crease pattern. A crease pattern for an origami crane can be found in Fig 1c. The creases are either pointing away or towards the folder. Those folds are called valley and mountain folds respectively.

A traditional paper airplane is a static origami structure, once folded the paper stays folded the same. However dynamic origami also exists, an example of dynamic origami is the paper crane, which by pulling and pushing its tail will start to flap its wings. Notice that one translational energy (the tail being pulled) led to rotational energy (wings go down). Origami engineering uses this energy translation and flexibility between folding configurations to its advantage to solve engineering problems or create consumer products [22] [43] [38].

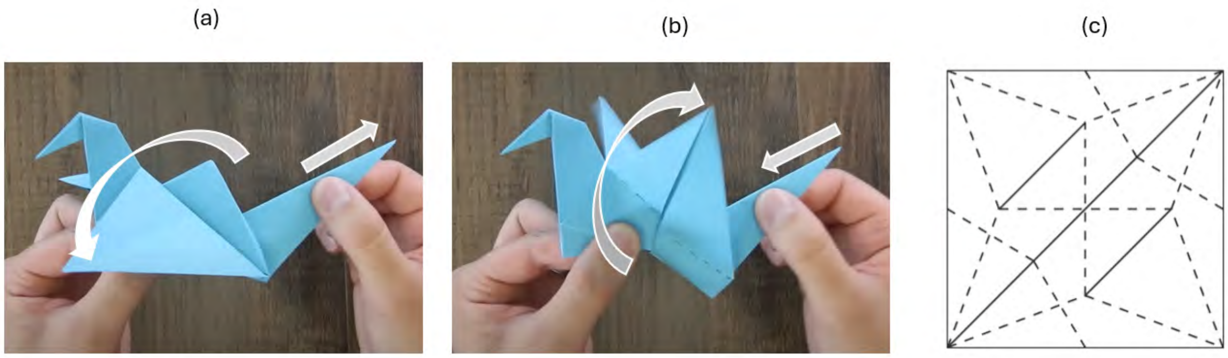

Figure 1: a and b: pictures of origami crane flapping its wings [6]. c: crease pattern of an origami crane, with mountain and valley folds [7]

A better-known application of origami engineering is the solar panels on satellites. During launch, the panels are folded compactly to reduce space. Once the satellite is in orbit the folds of the solar panel are undone creating a flat piece of solar panel. When looking at images of satellites the crease pattern is actually visible, as every separation in the solar panel is a hinge, or in origami terms a fold. Copying this crease pattern onto a sheet of paper allows the shape of the solar-panels to be copied, see Fig 2. this figure also shows well how origami patterns work on all scales, without changing the crease pattern. But origami engineering is not only limited to space engineering, it is used in many products from airbags to even deployable ballistic barriers [16] [51].

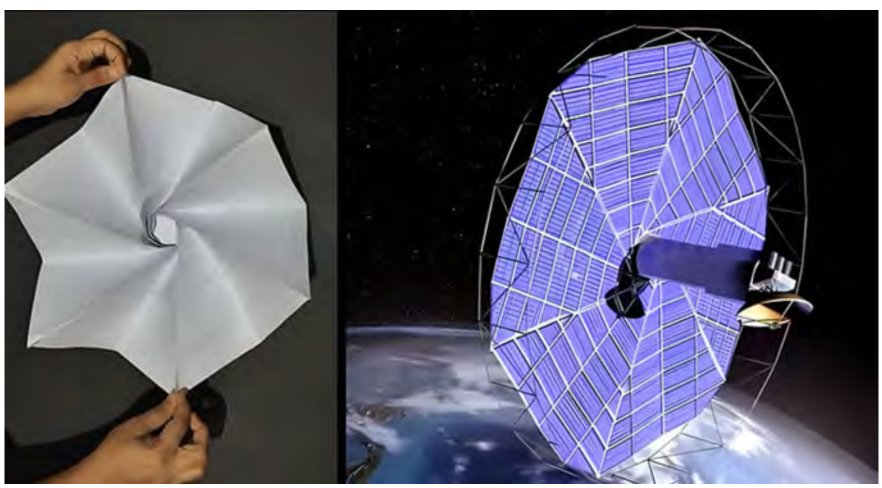

Figure 2: Picture showing how origami engineering is used in satalites and how their crease pattern can be recreated with paper.

2.3 Origami tesselations

Instead of transforming a sheet of paper into different shapes, it is also possible to add folds in such a way as to change the material properties of the paper. This is done via tesselations, one crease pattern repeated over the entire plane of paper. During this thesis, many tesselations were considered but the most of interest were: The waterbomb, Lang Oval Tesselation, the Hoffman waterbomb, the Hoffman stars-triangles, and The Resch Triangle tesselation. These patterns can be seen in Fig 3 As a dipole magnet inside a uniform magnetic field does not create a force, only a torque (more on this in chapter 2.5). Rotations inside the folding pattern such as the squares in the Hoffman waterbomb tesselation, were a plus. Furthermore, complexity and expansion were taken into account. The most interesting patterns were prototyped using standard origami paper to gain more insights into their workings. Although no conclusion was taken from this analysis, the knowledge about these patterns provided a toolbox for the concept phase.

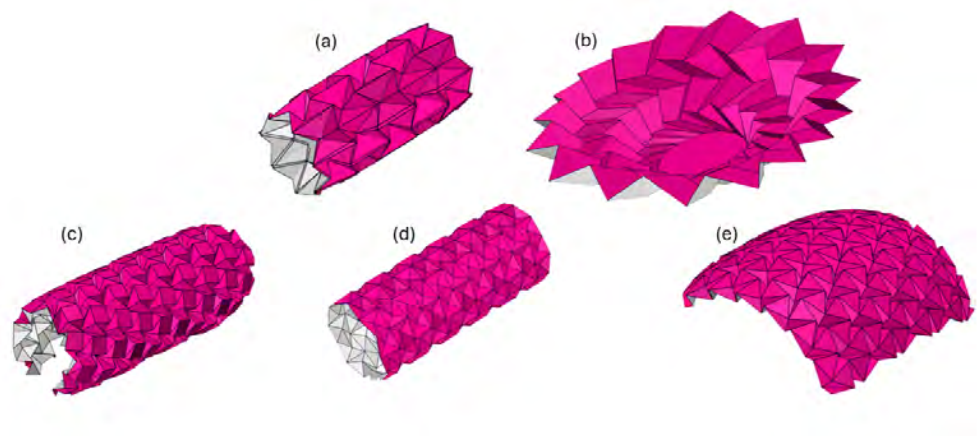

Figure 3: Tesselation patterns of interest for this thesis (a)Waterbomb, (b)Lang Oval Tesselation, (c)Hoffman waterbomb, (d)Hoffman star-triangles,(e)Resch triangle tesselation. [9]

2.4 Living hinges

Paper can easily be folded, however, in this thesis plastic is considered as an alternative material. Creating creases such that an otherwise stiff plastic material can fold has been in use for many years. Such a crease is called a living hinge and there are many types of living hinges. An example of a common living hinge is the hinge keeping the shampoo bottle and its cap connected. The plastic of the hinge, the top of the bottle, and the cap are all the same. However, only the hinge can be folded. This is done by making the crease less thick than the other region and is one of the simplest forms of a living hinge. More interesting patterns emerge with the other material living hinges are used, wood. Kits to create miniatures make use of living hinges to bend the normally straight pieces of wood in organic curves [4]. An example of such a kit and inspiration for this thesis can be found in Fig 4.

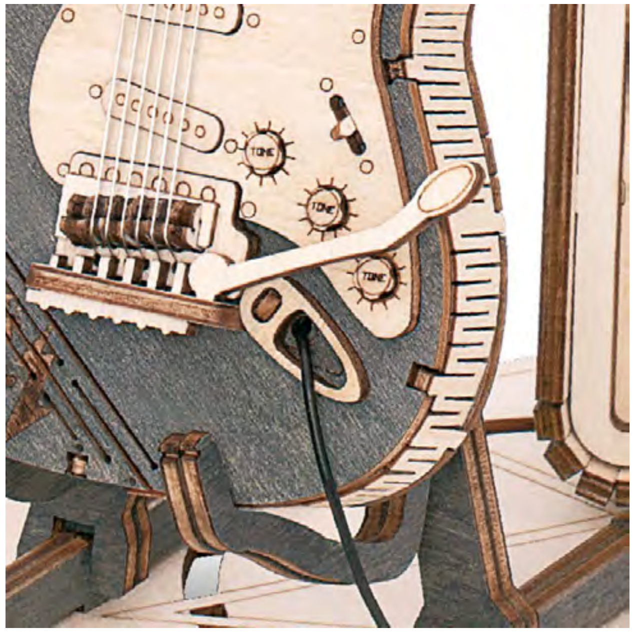

Figure 4: Living hinges as used in the Robotime electric guitar [10]

2.5 Magnetic actuation

All dynamic origami has a force that changes the configuration of the origami pattern to increase or decrease certain folds. These can take many shapes: for example motors inside the hinges for satalites [49], an explosion to unfold the airbags or, a hand pulling up the ballistic barrier.

The method of changing configuration in this thesis will be with dipole magnets inside a uniform magnetic field. Dipole magnets when placed inside a uniform magnetic field want to align with the magnetic field, creating a torque. Counterintuitively placing a magnet inside such a field does not create a force, meaning that the magnet does not want to move or fly away, it only wants to rotate. By placing magnets on certain panels of the origami a torque inside the origami system is created and the structure changes to the desired configuration.

To achieve a uniform magnetic field in this thesis Helmholtz coils are used. This setup consists of two identical electromagnets placed in line with each other. In the area between these two magnets, a close-to-uniform magnetic field is created.

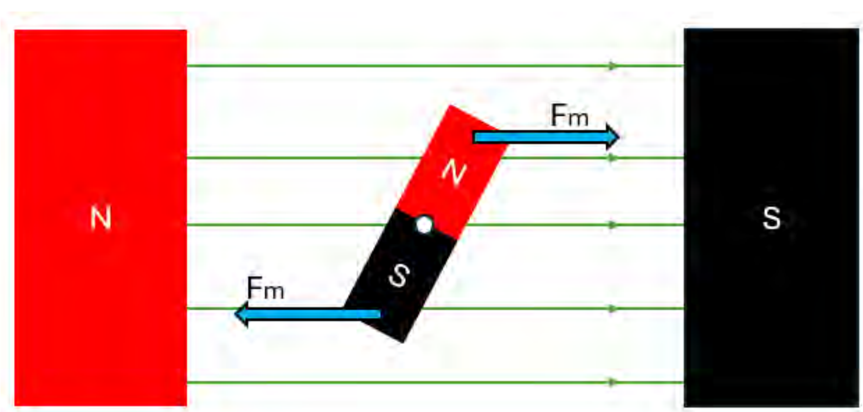

Figure 5: Diagram showing the forces created by the bipolar magnet inside a uniform magnetic field resulting in the rotation of the magnet.

2.6 AAA

An Abdominal Aortic Aneurysm (AAA) is a widening of the abdominal Aorta. When the aorta has a dilation in diameter of at least 50% relative to its expected diameter it is defined as an AAA [36]. Estimates on prevalence lie between one and twelve percent, with a median of 5 percent [53]. However, this number increases to 8% for men above 65 years [45]. There are also a lot of deaths due to AAA. In the USA alone 6.300 people die every year due to complications from AAA [53].

There are two methods of treating AAA, open surgical AAA repair and endovascular repair (EVAR). EVAR has been on the scene since the 1990s and is considered the preferred method of treating AAA, due to its lower mortality rate [28]. The treatment is a minimally invasive surgery (MIS) where a stent is positioned to the aneurysm via the leg. This stent reduces the pressure on the aortic wall and thus prevents the aortic wall from bursting. EVAR uses less anaesthesia and reduces compilations in patients with chronic obstructive pulmonary disease and or kidney disease, however when an aneurysm does not fulfil specific standards an open surgical repair has to be done. This treatment, introduced in the 1950s, consists of the surgeon opening the chest of the patient, opening the aorta and sewing a tube similar in shape and size to a healthy aorta inside the aneurysm. This procedure is more intensive for the patient and takes longer than EVAR, but is needed if EVAR is no option.

A third treatment method using drugs has been in development over the past few years. However, as this method's effectiveness is currently seen as controversial or inconclusive, it is not taken into account for this thesis [40]. The focus of this paper will be on making the EVAR procedure more easy and reducing the time of operation. One of the major difficulties during the procedure is placing the guidewire in side arteries [54]. This is currently done with a long wire and takes skill and patience to do correctly. The design proposed in this thesis could provide an easier alternative.

2.7 State of the art

Origami robots to be used inside the human body for medical applications do exist. For example, a magnetically actuated origami robot designed to be ingested. The little robot would expand inside the stomach and with the magnetic fields would be controlled to carry out underwater manoeuvres to remove a button battery, burned inside the stomach [42].

Another origami robot for the digestive tract is the capsule endoscope which can be seen in Fig X. This. This design uses origami to control the direction of movement, when the origami pattern is folded the capsule is propelled forward through the intestinal peristalsis. When the structure is unfolded the origami structure causes the intestinal peristalsis to push the capsule in the opposite direction, although the method of controlling the origami has not been tested, one of the proposals is to actuate the origami via a magnetic field [27].

These examples show how magnetic actuated origami can be used in practice. A more conceptual method is the magnetic origami spring robotic system. This device uses the torque created by two permanent magnets inside a uniform magnetic field to expand and collapse an origami structure [61].

The lack of origami capsule robot devices for endovascular systems suggests that origami might not be a good solution or even possible inside the endovascular system. However, an intracardiac magnetic resonance imaging (ICMRI) catheter was redesigned using origami. The system not only became more compact the new design showed improvements [55]. The structure was however not actuated via a magnetic field, as that would disrupt the magnetic resonance imaging.

The last device to mention in this state-of-the-art section is the master thesis of G.M. van Vliet. The device has fins on the outside of the capsule positioned as the thread of a screw. The idea is that when the capsule is rotated, it moves forward through the aorta like a bolt moving through a nut. The system however damages the aorta too much potentially due to sliding and the fins being too stiff. [57].

These devices were put inside a Venn diagram, see Fig 6. This Venn diagram shows clearly the problem with the current state of the art. A device that is origami-based and has magnetic actuation, and is designed for endovascular use seems to not yet have been proposed. There are however already devices that have 2 of the 3 traits, which can be used as inspiration.

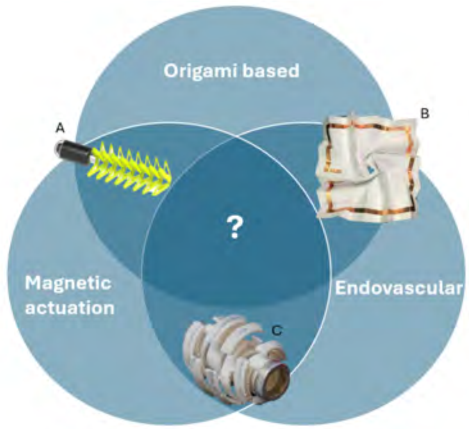

Figure 6: Venn Diagram visualising the current state of the art of magnetically actuated, origami-based, endovascular devices. A: Magnetically actuated, origami-inspired endoscope capsule. B: Origami-based ICMRI cathether. C: Compliant magnetic capsule robot to traverse the aorta. [27] [55] [57]

2.8 Mass-spring-damper model

To model the behaviour of the modules a Mass-Spring-Damper (MSD) model is used. As the name suggests an MSD model consists of a virtual mass connected to the ground via a spring and a damper. The mass in the model used in this thesis has 1 Degree Of Freedom (DOF) meaning that the mass can only move up and down, this displacement will be called x. The last part of the MDSM model is an external force F acting on the mass. This model is visualised in Fig 7.

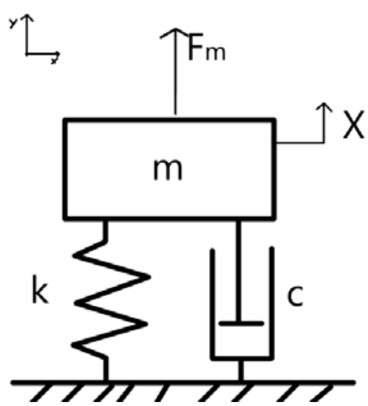

Figure 7: Sketch of a 1 DOF Mass-Spring-Damper Model

The spring with stiffness k pushes and pulls the mass towards a desired point. However, without a damper, the mass will always be oscillating. This is similar to a pendulum swing trying to get the ball to the lowest point, but constantly overshooting resulting in the oscillating behaviour the swing is known for. The damper takes energy out of the system and slows down the mass, stopping the oscillation of the mass. For the pendulum swing example, the damper is air, reducing the speed of the swing and taking energy out of the system and converting it into the air, eventually resulting in the swing hanging statically at the bottom of the rope.

Using the equation of motion of the MSD model predictions can be made on the behaviour of the system. This can be done by analysing the damping ratio, this ratio is calculated as follows:

$$F_m kxc\dot{x} = m\ddot{x} \tag{1}$$

$$\zeta = \frac{c}{2m\omega_n} \quad \text{where} \quad \omega_n = \frac{k}{m} \tag{2}$$

The system can be undamped ($\zeta = 0$), underdamped($\zeta < 1$), critically damped($\zeta = 1$), or overdamped ($\zeta > 1$). To calculate the movement of the model a Matlab script made by Jaison Kim VT was used as the basis and modified to fit the desired model [34].

2.9 Additive Manufacturing

Additive Manufacturing (AM) better known as 3D printing is a relatively new production process that formerly was known as rapid prototyping. Over the years users realised that this technology has more uses than only rapid prototyping and was thus rebranded to additive manufacturing [**?**]. There are different types of AM machines but all create a product by adding material, thus the name additive manufacturing.

To produce an object using AM an object is made in 3d software. This object is converted to a stereolithography (STL) file approximating the object made in the 3d software with triangles. Using slicer software, the STL file is then sliced into layers with each layer containing the information of how that specific layer needs to be printed [58]. The 3d printer then prints each of those layers one by one resulting in a physical version of the digitally drawn object.

One of the reasons additive manufacturing fits so well in this thesis is because developing a scaled up or scaled down version of an object is easy. this makes additive manufacturing a good match with origami, what also can be scaled to any size without much problem. As mentioned earlier many different versions of AM exist most common is the FDM printer based on melting a solid so it can be placed on the printer bed. But other versions are based on the polymerisation of a liquid using light or melting powder particles together using a high-powered laser [26] [50]. In this thesis, the FDM printer "Bambu Lab A1 mini" will be used to produce parts for the prototype. *Benefits of AM?

Table 1: Design Requirements for origami magnetic capsule robot

Requirements		Description
R1	Outer diameter adaptability	Outer diameter must be able to fluctuate 16%
R2	Aortic wall safety	Pressure generated must not rupture the aorta.
R3	Locomotion	System must move through the aorta in a controlled manner
R4	Continued blood flow	System must allow blood flow and reduce pressure drop.
R5	Failure rate	Design must be simple yet strong enough to reduce chance of failure
R6	Biocompatibility	Material and shape must not induce an immune reaction in the body.
R7	Simplicity	For production and failure rate as few parts as possible must be used
R8	Origami Engineering	Design must make use of origami engineering to find a solution.
R9	Magnetic actuation	Design must be controlled wirelessly via magnetic actuation.

3 Preliminary Design

In this chapter, the preliminary design will be discussed. Based on the state of the art and the design problem, the requirements were set as design boundaries for this project. This is followed by the concept development and the decisions that lead to the final design.

3.1 Requirements

Based on the problem described in the introduction and the devices brought forward in the state of the art, nine requirements were created. This chapter will go into the details of these requirements, but a summary can be found in Table 1.

R1. Outer diameter adaptability The diameter of the Aorta fluctuates both dynamically due to the cardiac cycle and statically due to the building structure of the aorta. A study from 2019 [32] researched these fluctuations. By taking the maximum diameter of the aorta (proximal-Asc) during diastole (34.10 mm) and the minimum diameter (distal-asc) during systole (28.77mm) and normalising these two values the contraction factor can be calculated to be 0.84. Thus the concept must have an outer diameter of 31.44mm and at least be able to adjust its outer diameter with ±8%.

R2. Aorta wall safety A burst in the aorta wall would be catastrophic, Bogdan Ciszek et al. found that the burst pressure of the aortic wall was on average 2.24E5N/m^2 with the outer limits being 1.14E5 and 4.36E5 N/m^3 [18]. With a little bit of safety margin but taking into account that the system is still just a prototype a maximum of $1.0E5N/m^2$ is set as a requirement.

R3. Locomotion Navigation of the capsule is an important part of the design, the system should be able to move through the aorta in a controlled manner.

R4. Continued blood flow The aorta is an important part of the blood circulation system and the impact of the concept on blood flow should be mitigated. A study in 2022 [14] simulated different blockages of the aorta and found that a blockage of over 35% had a significant impact on blood pressure. A maximum of 35% blockage will be taken as a goal, however, in further research, the maximum allowed pressure drop must be calculated.

R5. Failure rate As the aorta is such an important part of the human body a failure of the capsule of any sort can be catastrophic and cost a human life. The exact failure frequency does not matter yet, as this can not be tested during this thesis. The requirement is however still taken into account during the design process and must be as low as possible.

R6. Biocompatability The immune system of a human body does not like foreign objects. Although the capsule is not meant to be in the human body for long periods, the immune system should not activate or attack the capsule. To do this a coating can be used of biocompatible material and sharp edges must be reduced to the bare minimum.

R7. Simplicity A simple design is often the best, in this thesis that is for two reasons. First, fewer parts mean fewer points of failure. So to keep the failure rate as low the design must have as few parts as possible. Second, every extra step that is needed in the production process because of extra parts costs time and increases the chance of errors happening during production. Overall, there is no hard limit to the maximum number of parts allowed, but as a guideline, the thesis aims to keep the number of parts below 100.

R8. Use origami engineering The goal of this research is to set a step forward in origami engineering for MIS. The knowledge gained by developing this system with origami engineering is thus valuable.

R9. use only magnetic actuation Although the system will most likely pull a guidewire, the requirement for the system is that it can be wirelessly controlled only by adjusting a uniform magnetic field in which the system is placed.

3.2 Ideation

Following the requirements and the state of art analysis. Four key variables were defined. Method of locomotion, Aortic adaptability, base structure of the design, and method of actuation. These variables were put in a morphological diagram and for each variable, at least three solutions were found. This diagram can be found in appendix 9.1. Parallel to that insight into existing tesselating origami patterns was investigated via literature research. These origami patterns were graded on their potential use. The names used were the names given by origamisimulator.org.

3.3 Concepts

The concept phase included the development of 3 concepts. These were derived from the morphological chart, described in the previous chapter. These concepts all use a different method of locomotion and were deliberetely designed to be as unique from each other as possible.

3.3.1 Self-propelled vine robot

The first uses the treadmill method for locomotion. This solution was inspired by the vine robot developed in 2020 by researchers at Stanford University [20], this robot can locomote by expanding its tip without having to move itself. It does so by feeding itself new material via the inside. It should be possible however to feed itself just as Toroflux, a toy from 2010 [31]. And as it happens such a robot was presented in 2022 that used this technique with an internal robot [48]. This proves that this is a valid locomotion technique. The self-propelled vine robot concept also uses the inflated tube system, to adjust its radius to the desired value. Using the origami kaleidocycle pattern was also considered, this pattern can be seen in Fig 8. However, as this pattern would be more difficult to expand or retract radially was not chosen over the inflated tube.

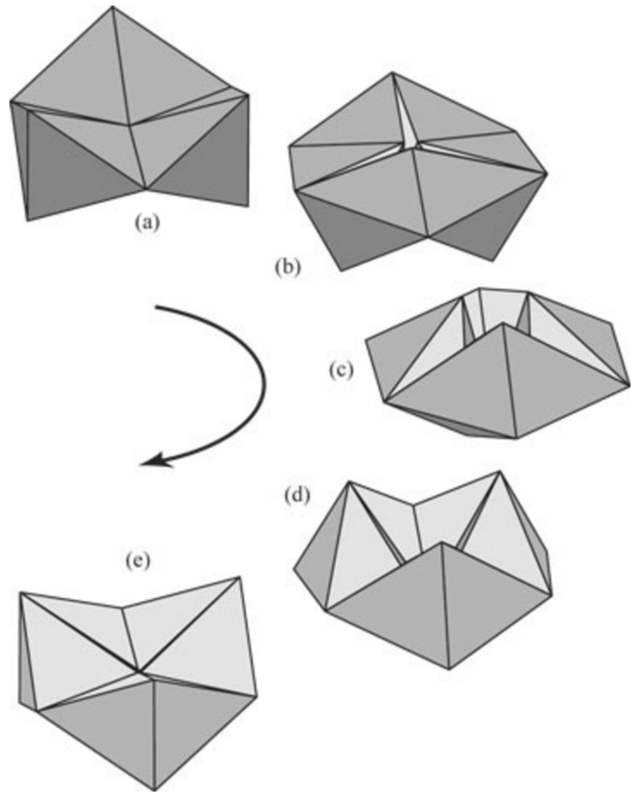

Figure 8: Step-by-step visualisation of the working of the koleidocycle, starting with a, then b, until e. After e the cycle starts again with a. [23]

The self-propelled vine robot would be actuated by placing small magnets on the tube, by oscillating a magnetic field at just the right time the system would move in the desired direction. A sketch of the concept can be found in Fig 9.

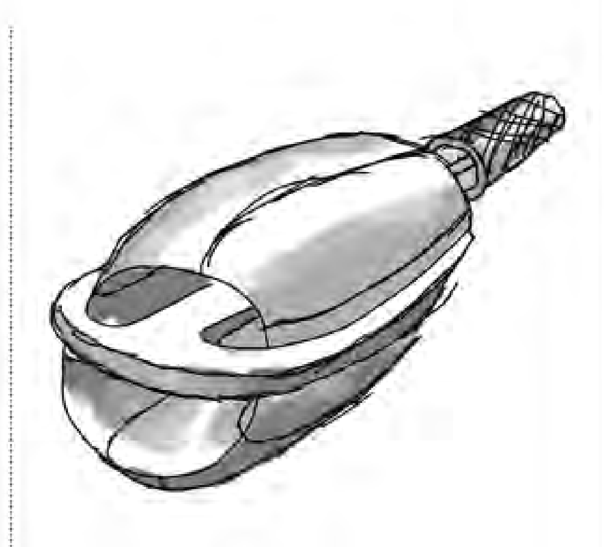

Figure 9: Sketch of the self-propelled vine robot pulling a stent

3.3.2 Popping screwthread

The second concept was inspired by the screw design of G.M. van Vliet [57]. His device rotates axially through the arteries, and fins on the outside of this device slide the device forward as a bolt sliding through a nut. The popping screwthread concept uses the same locomotion method. Having a body that rotates axially with fins on the outside. However, instead of rigid fins these fins can collapse for easier placement and retrieval from the human body, and more subtle actuation prevents damage from happening on the arteries. A sketch of this method can be found in Fig 10.

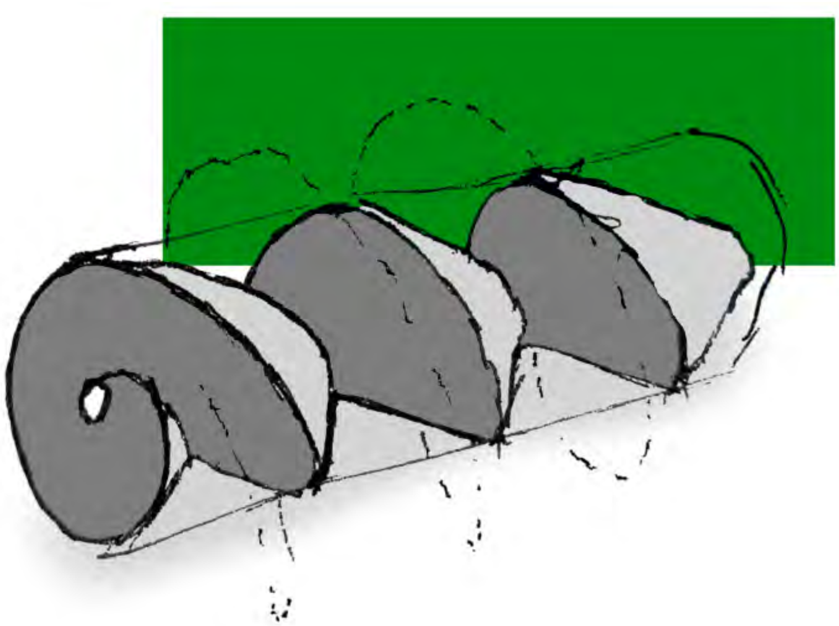

Figure 10: Sketch of the popping screwthread concept

3.3.3 Negative-poison ratio worm

The last concept was the negative poison ratio worm, inspired by a paper exploring negative poison ratio origami structures to create a worm-like robot [24]. But what is a negative Poisson ratio structure? Most objects when stretched in one direction, contract perpendicular to this force. A good example would be a rubber band which when pulled becomes thinner. A negative Poisson ratio object does the opposite, when stretched in one direction it expands perpendicular to this force. Making it look similar to a balloon.

The previously mentioned paper adds several of these negative Poisson ratio origami structures next to each other and is able to control them separately. This allows the researchers to create a wormlike peristalsis movement. However, the researchers use motors to actuate these structures which is not possible for the purpose of this thesis. So this concept is a scaled-down version of that worm with magnets actuating the waterbomb origami structure. A concept sketch was made and can be seen in Fig 11. It consists of 6 modules that have a negative poison ratio, 3 are inflated in a positive magnetic field, and the other 3 are collapsed inside the magnetic field. This switches when the magnetic field is inverted.

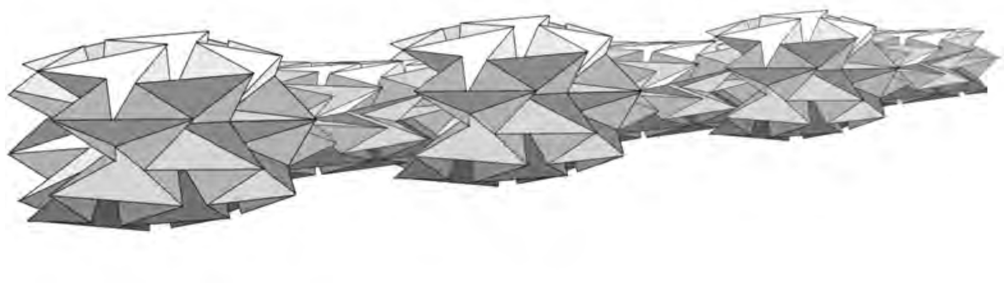

Figure 11: Early concept sketch of the Negative-poison ratio worm, consisting of 6 identical modules.

3.4 Choosing a concept to continue

The first concept to fall was the screw thread concept. This is because in the discussion of his research, Vliet brings up that the device will most likely heavily damage the aorta, he proposes several reasons, the device has too much surface roughness, too high stiffness in the fins and/or low compliance with the aortic wall. The popping screwthread concept would most likely walk into the same problems. Although these could potentially be solved by optimising the material and dimensions, the other two concepts do not require sliding over the aortic wall and thus are assumed to be a lot less damaging.

Choosing between the vine and the worm concept was more challenging. But due to its complexity in integrating origami and no clear method to reduce its outer diameter the vine concept was scrapped as well.

This left only the worm robot. But with the first few paper prototypes made, the problem arose that although the waterbomb did expand 2.5 times radially it only expanded 1.01 times axially. This very little expansion axially would not allow for proper locomotion. This happened due to a misinterpretation of the original worm paper, which would not be discovered until much later in the thesis.

This discrepancy in expansion would however hold the key to the final design. As the waterbomb has a near 0 expansion axially then by adding a module which almost does not expand radially but does expand axially the same locomotion is possible. This solution also, almost paradoxically, allows for fewer modules to be used. As for locomotion, only three modules would be needed; two modules that alternate to grip the wall of the aorta, and one module that displaces the module that has no grip. For visualisation, a sketch of this final concept can be seen in Fig 12.

The two modules that alternate with grip on the aorto need to expand radially and will be referred to as the First Radial Module (RM1) and Second Radial Module (RM2). Radial Module (RM) is used when non-specifically referring to either RM1 or RM2. Connecting and displacing the RM's is a module that needs to be able to expand axially, so this module will be referred to as Axial Module (AXM).

4 Final design

The final design consists of three parts: two modules that can expand radially connected by one module that can expand axially, as sketched in Figure 12.

This chapter starts with a deeper analysis of the locomotion methods that are possible with this setup. After that additional requirements are described per module. Because, to make this new design and locomotion method work additional requirements are needed. These requirements and first prototypes lead to decisions in origami pattern, magnet placement, and the material. Which will be described in detail at the end of this chapter.

4.1 Locomotion

To determine how the device would move, first, the ideal sequence of expansions was identified, what would be the best sequence if there were no limitations? Assuming all modules are collapsed, first, RM1 expands and clamps the aorta. Then AXM pushes RM2 forward. When RM2 is in place it expands and clamps. RM1

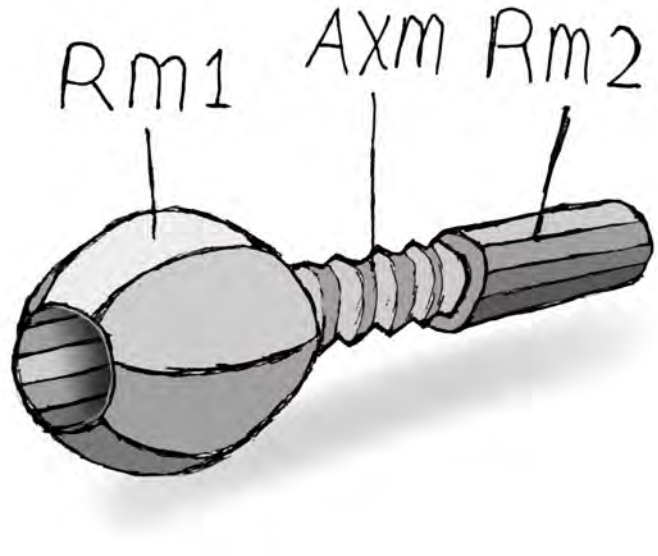

Figure 12: Sketch of the final concept, consisting of the three modules: RM1, AXM, and RM2

is then deflated which, when fully deflated, is pulled towards RM2 by the retracting AXM. This process is repeated until the device is at the desired location. This is visualised in Fig 15a.

4.1.1 Control

In this ideal sequence, all segments expansion can be independently controlled, thus three inputs are required. Control can be seen as three levers each controlling the expansion and retraction of one of the modules. It is however not possible to recreate these three levers with just a magnetic field. The direction of the magnetic field is in line with the symmetry axis of the device, see Additional Requirements 4.2. This means that there are only two levers available: frequency and magnitude. Frequency means the number of times the magnetic field switches its polarity per second. This behaviour can induce induction and generate a small amount of electricity and/or heat to a receiving coil.

Magnitude is not as simple as frequency, as instead of a lever it can better be seen as a switch that can switch between positive, negative and zero magnetic fields. The reason using a variable magnitude is the same as a switch is as follows. If for example RM1 is completely expanded at 25mT and is fully retracted at -25mT. Whereas RM2 requires the opposite -25mT for expansion and 25mT for collapse. While the AXM requires at least 50mT to expand or -50mT to collapse. Knowing these values the first thing to do is to expand RM1 and collapse the second, so the field is set to 25mT. As RM1 reaches the end of expansion it gets a grip on the aorta, and RM2 loses grip immediately. AXM expands for 75% without the grip of either RM so both RM modules are pushed away equally, meaning the center of mass of the device stays the same. But now that RM1 has grip the AXM needs to expand further to push RM2 forward. So the magnetic field is set to 50mT and the AXM expands nicely. However now RM2 needs to expand, so the field needs to be set at -25mT. To get to this value, the field must decrease from 50mT to 25mT to 0mT to end at -25mT. But the first step causes a problem, as decreasing the magnetic field from 50mT to 25mT will just undo the expansion from the AXM that was just done. Thus RM2 will expand at the exact same location it was in the previous cycle, which is also true for RM1. There is one thing which could make such a system work and that is history. In this example, the assumption is made that a module will always be at the same expansion rate dependent only on the magnetic field. So no matter the situation, if the field is 25mT the AXM is always expanded 75%. However, if the module is stiffer to close than to open, then there is a difference in expansion between the two 25mT points for example 73% when opening and 78% when closing. This means that practically AXM has a netto expansion of 5% while RM1 has grip. This means that netto RM2 is displaced with this same value and thus displacement of the device will happen. In chapter 5 the existence of this behaviour with history is proven although it is not significant.

To summarise, using a proportional magnetic field to actuate the modules based on different stiffnesses is not possible. Thus the magnetic field can be seen as positive, negative or, off.

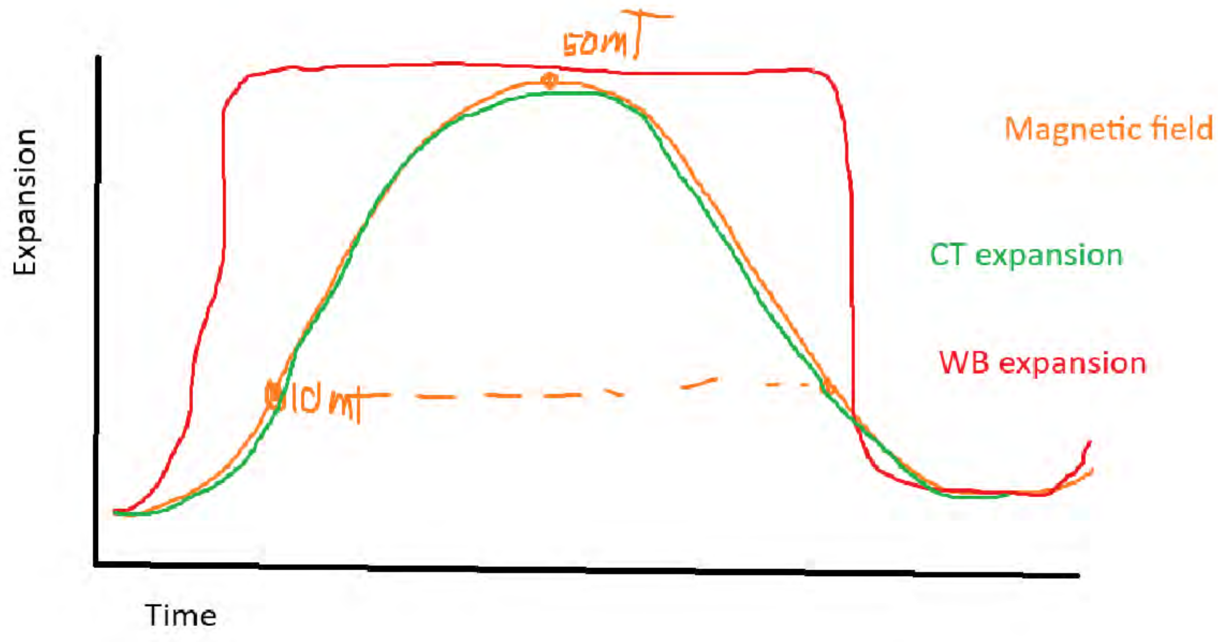

Figure 13: Sketch of predicted movement during amplitude-sequence method

4.1.2 Sequences

Different sequences have been explored and put in a locomotion diagram which can be seen in Fig 15. This subchapter will first tell you how to read the diagram and then go into detail about the different possible methods.

In the diagram all 3 segments are assigned a number between 0 and 1 correlated to the state of that module so 1-0-0 should be read RM1 = fully extended. AXM and RM2 are totally collapsed. This coding is visualised in Fig 14. The colour code of the locomotion diagram is as follows: the purple and green squares indicate whether the magnetic field is positive or negative. The red border indicates that the field is using conduction to heat up a desired part, where as the blue border indicates it has been turned off.

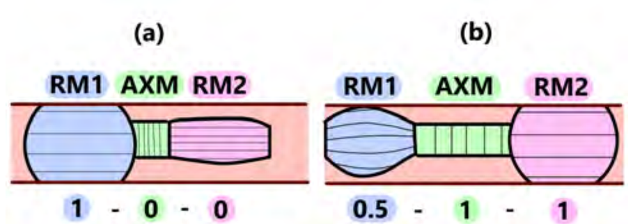

Figure 14: Visualisation of code used in locomotion diagram with two examples. (a) RM1 expanded, AXM and RM2 collapsed. (b)RM1 partially expanded, AXM and RM2 expanded

Ideal sequence As mentioned in the beginning Fig 15a. shows the ideal 3DOF no constriction pattern. Pattern B was the first attempt to a 1 DOF sequence. All segments open when put under the same magnetic field, however with different stifnesss and dampings a delay causes the first to be opened then the second and at last the third. When put under an inverse magnetic field this once again happens but in reverse, the first one closes then the second and at last the third. This sequence pushes RM2 when RM1 has grip and retracts RM1 when RM2 has grip so the device will displace. However, this method has a downfall, during the cycle there is a moment in which both the first and third segments are not clamping. As this could result in the robot moving with the bloodstream this is not desired.

2 DOF sequence The next step was to add a DOF. This was done by adding an induction coil that heats the creases of the AXM, if the ASM is made of memory shape polymer the segment can be turned on to react to the magnetic field. this can be seen in Fig15c. Assume RM1 and AXM open during a positive magnetic field while RM2 closes under the same field. However AXM only changes state if the induction coils heat up the creases of the module. A method of locomotion is as follows, starting with a positive magnetic field without induction, RM1 opens without AXM. Then AXM is heated up and folds open under the already present magnetic field. It is then cooled the hinge stiffens once again. The magnetic field then switches causing RM1 to collapse and RM2 to open. AXM remains open as it is stiff. When RM2 has grip, AXM is heated which causes it to close under the magnetic field and pulls RM1 to RM2. AXM is cooled and the magnetic field becomes positive again after which the cycle repeats. This method would work but the usage of MSP adds complexity to the device, which increases failure modes and the complexity of reducing its size.

Second 1 DOF sequence The final method D, was done by assuming different expansion speeds for different modules. Specifically, AXM opens and closes much slower than RM1 and RM2. The cycle would be as follows. The magnetic field starts positive opening RM1 and AXM. However, when AXM is at full expansion and gets traction AXM is not nearly done with expanding and pushes with the remaining time RM2 forward. Then the magnetic field is inversed and RM1 and RM2 quickly switch states. AXM which is still slower pulls once RM2 gets traction segment one to RM2. This then repeats over and over. In this example AXM is quicker than RM1 and RM2. However as long as these speeds are not the same the technique should work, inversing (so RM1 and RM2 are quicker then AXM) would make the device move backwards. But as there is no front or back yet to the device as long as the expansion speeds are not equal the system should move.

*insert figure with sketches of the device performing chosen locomotion method.

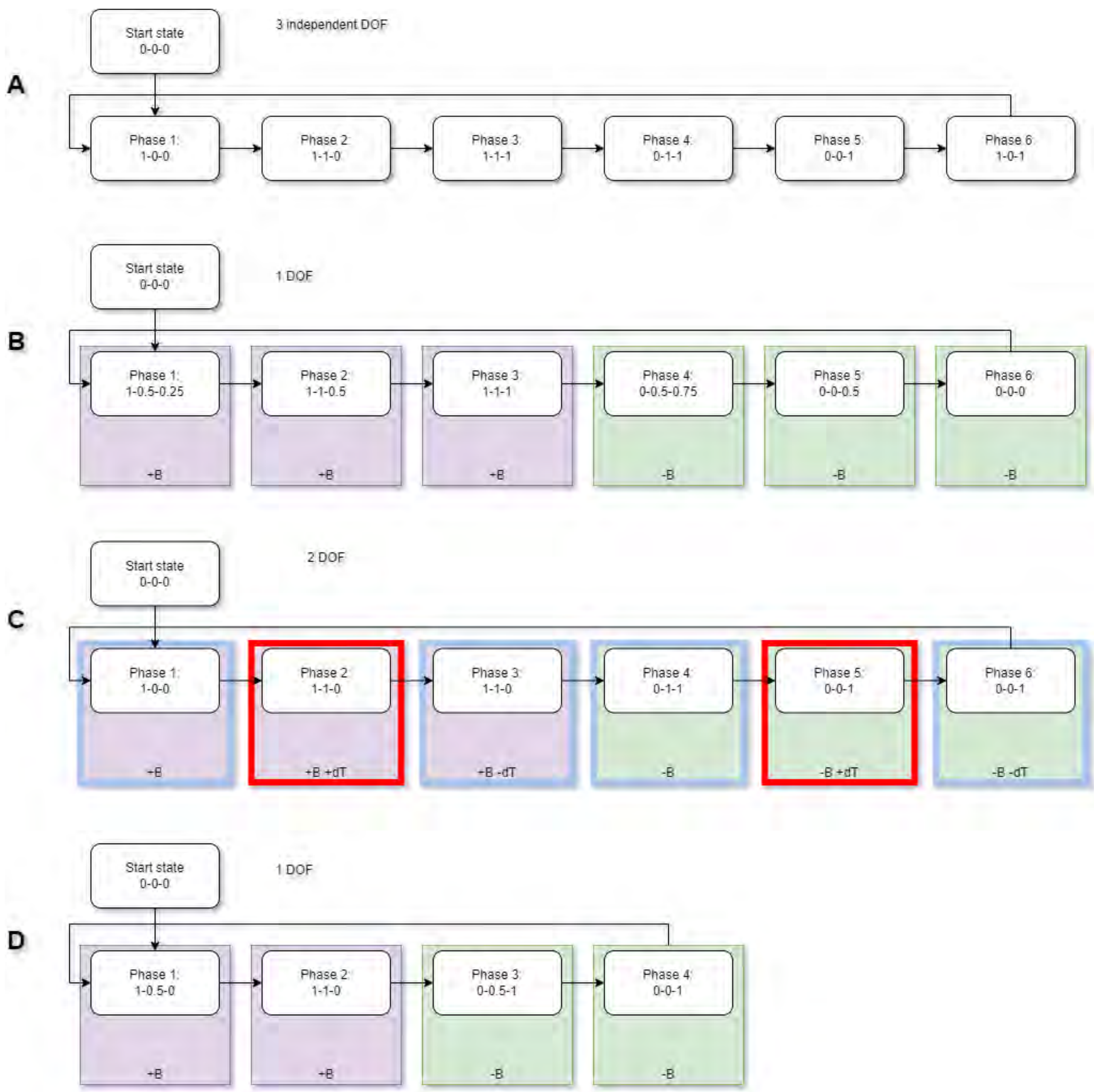

Figure 15: Explored locomotion sequences. (a) Ideal sequence.(b)First 1 DOF sequence (c)2 DOF sequence (d)Second 1 DOF sequence

4.2 Additional Requirements

To enable this final design and locomotion technique, additional requirements were set up. The requirements can be found in Table 2, in this chapter these added the details of these requirements can be found. It is important to make clear that these requirements are in addition to requirements found in Table 1, the original requirements are still valid.

4.2.1 Requirements for RM

rm-R1 Radial Expansion This requirement at a glance seems very similar to requirement R1 Outer diameter adaptability. But the reasoning and fluctuation value are very different. To enable locomotion the RM needs

Table 2: Additional Requirements for origami magnetic capsule robot

Requirements		Description
	Radial Module	
rm-R1	Radial expansion	For locomotion device needs to expand 2x radially.
rm-R2	No axial expansion	For simplicity no axial expansion is prefered
rm-R3	Module interface	The module must be able to connect to the collapsable tower.
rm-R4	Field along symmetry axis	Actuation only possible via magnetic field along symmetry axis.
rm-R5	Quick expansion	Needs to expand and retract quicker than the collapsable tower
	Axial module	
axm-R1	Axial expansion	Needs to expand and retract slower than waterbomb.
axm-R2	No radial expansion	For simplicity no radial expansion is preferred.
axm-R3	Module interface	The module must be able to connect to the waterbomb.
axm-R4	Field along symmetry axis	Actuation only possible via magnetic field along symmetry axis.
axm-R5	Slow expansion	Needs to expand and retract slower than the waterbomb.

to expand and retract radially. This is explained in chapter 4.1. This means that when the RM is expanded and gripping the wall, it needs to retract at least 16% to be certain that the RM has no more contact with the aortic walls. Calculated as follows $1 - \frac{\text{min. radius aorta}}{\text{max. radius aorta}}$ which is $1 - \frac{28.77}{34.10} = 15.63\% \approx 16\%$. In this thesis the expansion value is used more commenly, similarly calculated as the retraction value but switching the numerator and denominator the lowest expansion value to be certain that the RM touches the aorta is 19%. To be certain the device does not slide along the aorta an ambitious but possible expansion value of 100% (or retraction value of 50%) was set as a goal and requirement.

rm-R2 No axial expansion Why no axial expansion is required for the RM module can best be explained by analysing what would happen if there was axial expansion. If the device is seen as one unit the axial expansion is not a problem, the axial expansion of RM1 would in theory cancel out with the axial retraction of RM2. However, analysing at a modular scale it can be seen that the AXM is now rocking unnecessarily between the two RMs. This not only a loss of energy but could also increase the failure rate of the interfaces between the modules.

rm-R3 Module interface This requirement is more straightforward than the previous requirements. The RM module needs to be able to connect to the AXM module.

rm-R4 Field along the symmetry axis The final design requires the RM to expand in all radial directions simultaneously. A method to achieve this is to make the device radially symmetric just like for example a snowflake. Then with magnets on the origami pannels have a magnetic field run straight through the heart of the snowflake. This means that every arm (for the lack of a better word) of the snowflake receives the same magnetic field and thus should expand or retract in perfect synchrony. Something to note is that more arms are better, as the force is more evenly distributed and deviations in expansion between arms (due to production error for example) are less noticeable. However a minimum number of arms is not set as requirement as the device would work with both 3 arms or with 50. Just possibly without the previously mentioned advantages of having more arms.

rm-R5 Quick expansion As described in section 4.1 the locomotion method uses the difference in expansion speed between the RM and the AXM to generate displacement of the device. As the AXM needs to displace RM2 and thus has more inertia, and needs to expand over a larger distance. The goal is to have the RM be quicker in expansion than the AXM

4.2.2 Requirements for AXM

axm-R1 Axial Expansion The method of locomotion relies on the axial expansion of the AXM. Although in theory any expansion above 0% would be enough for locomotion, a low expansion rate would require more cycles for the same displacement with a larger expansion rate. A target rate of 100% expansion, or 50% reduction is set as target for this thesis.

axm-R2 No radial expansion Radial expansion inside the AXM means more displacements and thus more energy loss. Making the device less efficient and prone to a higher failure rate.

axm-R3 Module interface The AXM needs to connect to the RM on both sides and thus needs 2 interfaces for the other modules.

axm-R4 Field along symmetry axis Although on its own the AXM does not need this requirement. However as the RM requires it, the AXM has no other choice than to do the same.

axm-R5 Slow expansion See 'rm-R5 Quick expansion' for the explanation why the AXM needs to be slower than the RM.

4.3 Origami patterns

Now that the requirements are clear, different origami patterns can be explored and optimised.

4.3.1 Origami pattern for RM

For the RM, there were three origami patterns in the running. The waterbomb, the Lang Oval tesselation, and the Huffman's waterbomb. These patterns can be seen in Fig x. Starting with the Lang Oval Tesselation, two of these patterns would be connected via rods. The static core of the pattern would allow for an easy interface between modules, but due to the limited expansion rate and overall complex design the Lang Oval Tesselation was discarded.

The Huffman waterbomb was also close to glory as the rotating squares would make actuation via magnetic torque straightforward. However there are many places in this pattern that the paper needs to make several 180degree bends in a row. The thicker the material the more difficult it is to make these bends. Due to this the Huffman waterbomb was discard as well.

This leaves only the waterbomb in the race. glueing the waterbomb pattern into a tube creates two holes (or one if you study topology) which stay constant in radius. This is ideal for interfacing to the AXM. The first prototypes during Ideation showed that there is no axial expansion which is also a requirement fulfilled. By adjusting the number of tiles the expansion rate but also the sharpness of the angles can be controlled. Previous research used 3x8 tesselation [24]. However this would expand one column completely. For the magnetic actuation method this is not handy as more commplete expansion allows better use of the magnets. An additional column was added as well to increase the expansion rate but still allowing the pattern to fit on an A4 paper. So the final tesselation size is 4x9.

Using these fold lines results in a proper waterbomb, however every plane will get a thickness thicker than paper. The reason for this will be explained in chapter 4.4 Material. This thickness creates a problem for valley-folds as the two panels glued on top will collide, see Fig 16a. There are different solutions, the use of offset hinges to create one hinge for example [39]. Methodologies for creating thick-paneled origami patterns do exist [46] [47]. Applying these methodologies was however out of the scope of this research. And as the offset hinges add too much complexity a different solution was used. Every hinge was replaced by two hinges, with between it a channel. The difference can be seen in Fig 16b. This method is far from perfect and is only possible because of the flexibility of paper which creates where necessary additional fold lines. This additional bending does make the system less energy efficient and makes the device prone to a-symetry leading to unwanted behaviour can be seen in practise in chapter 5.5 Explaining the rotation. Where the channels intersect a hole is made, this reduces stiffness but is not actually necessary.

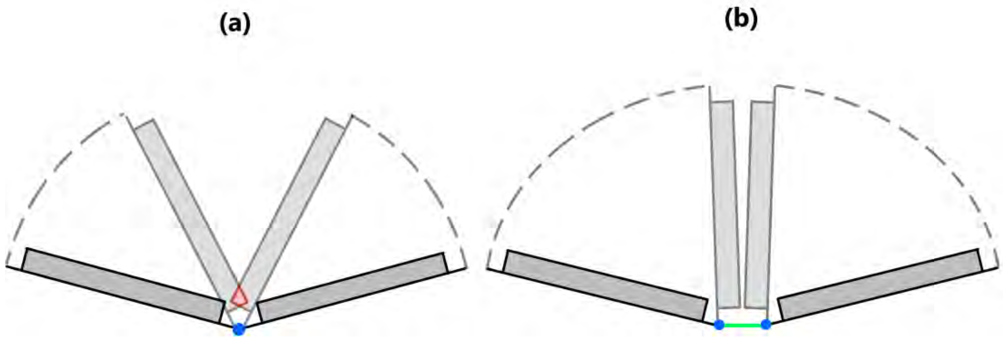

Figure 16: Visualisation to show that standard origami creases result in collisions (red), and how creating a channel (green) can prevent this

4.3.2 Origami pattern for AXM

The design of the AXM started in its simplest form, with 4 jigsaw folded arms seperately connecting the two other modules. A picture of this design can be found in Fig 17. This design is however, unstable. And although either retraction or expandsion can be easily achieved with magnets. Both is not possible.

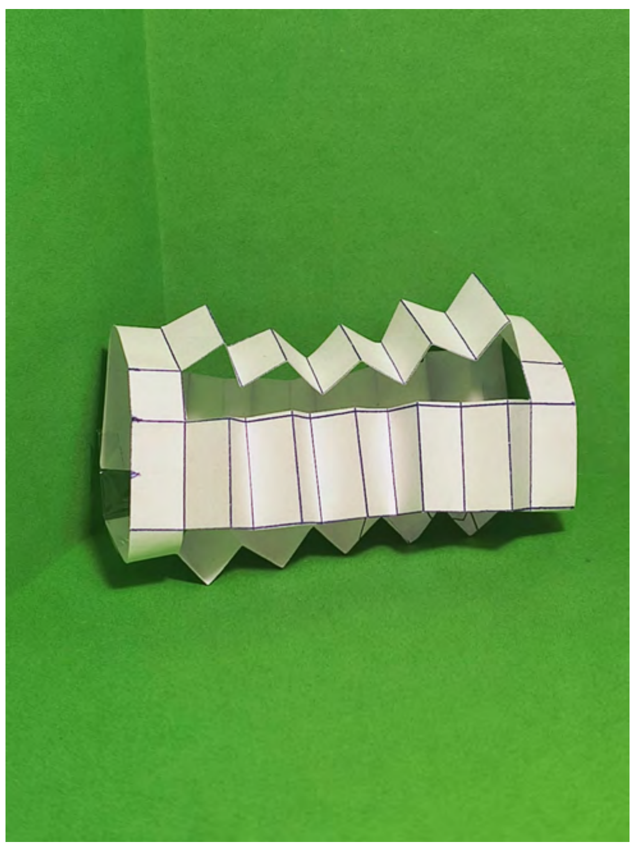

Figure 17: Picture of the first AXM design

With the focus on stability the next origami pattern explored was the Miuri tube. This tube can be seen in Fig 18. This pattern is a lot more stable than the first version, however as it has planar symmetry and not radial symmetry it is difficult to place magnets but also causes the ends of the tube to not remain static. Which makes connecting the AXM to a RM difficult.

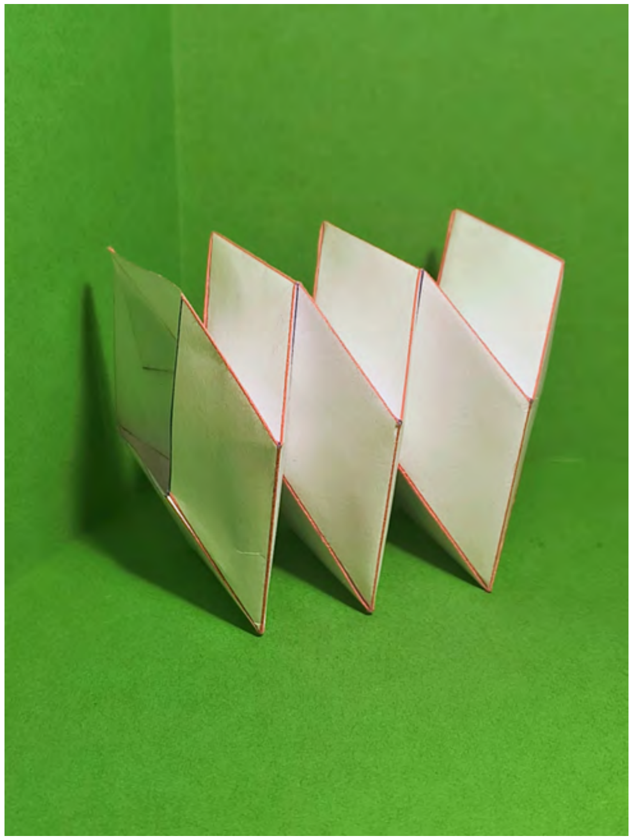

Figure 18: Picture of the Miuri tube.

Then during exploration for RM designs, the Huffman star-triangle tesselation was found. On origamisimulator.org this pattern folded in a tube without any axial expansion. So first several rings with different number of tesselations were made to determine if the pattern could be usefull. Such a ring can be found in Fig 19. With a theoretical expansion rate of 100% this seemed perfect. So some small scale magnet studies were already done on seperate tiles of this pattern, and with success. However, when trying to extend the ring to a tube the whole tube became too unstable and stiff, a picture of this tube can be seen in Fig 20. Thus also this design was discarded.

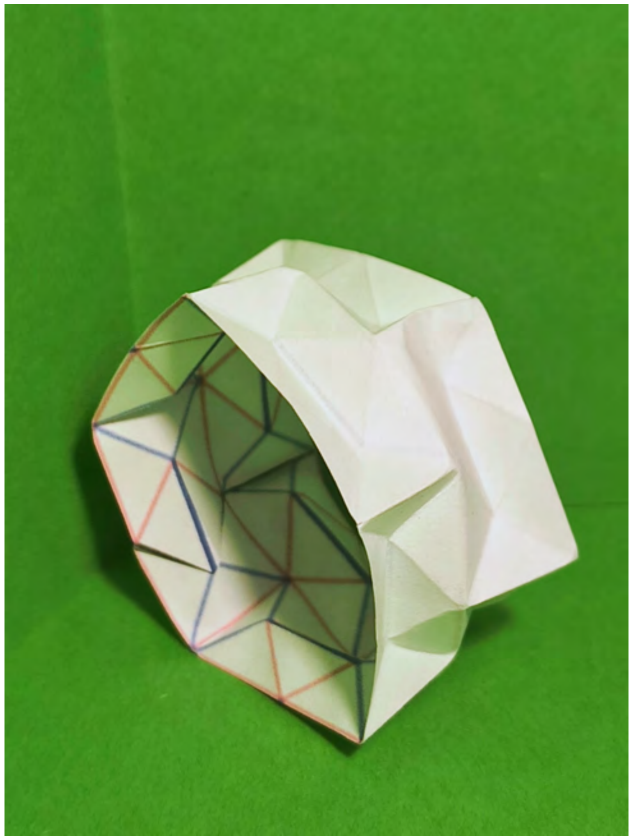

Figure 19: Picture of a 5x2 ring with the Huffman star-triangle tesselation.

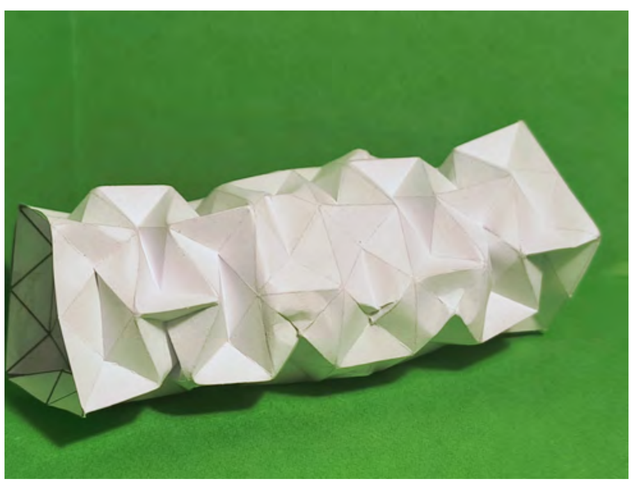

Figure 20: Picture of Huffman star-triangle tube, tesselation is 4x10

This leads to the pattern that would be used in the final design the ”collapsable tower dodecagon” (CT) [1]. This pattern showed a stable tube design with a static bottom and top, perfect for interfacing. The paper prototype, which can be seen in Fig 21, had an expansion rate of approximately 300%. However, as theAXMexpands the ends rotate with respect to each other. This is undesired as the rotation of one of the RM's could damage the aortic wall and costs energy. However, the ”Collapsible Tower Dodecagon V2 With Sectioned Folds” [2] came with a solution by mirroring every layer the rotation of the ends is netto zero. Meaning that the RMs will not rotate with respect to each other. The sectioned folds however were not necessary so these were removed without any issue. The resulting tube can be seen in Fig 21. This design is currently being researched on its impact mitigation capabilities, there the fold is called a Triangulated Cylindrical Origami (TCO) [60]. This thesis will however keep using the name Collapsable tower.

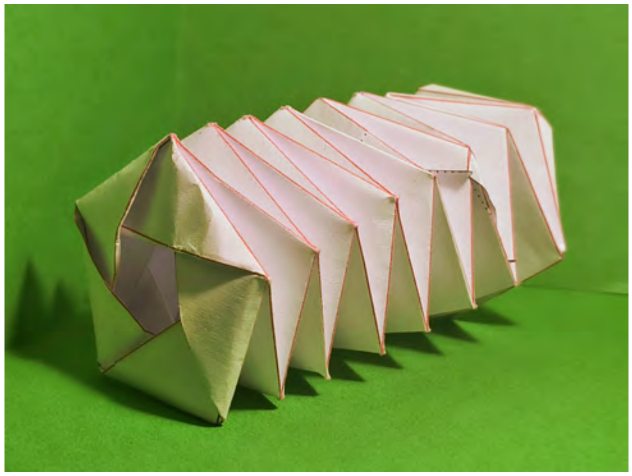

Figure 21: Picture of a 7 layered collapsable tower dodecagon

Figure 22: Picture of the "Collapsable Tower Dodecagon V2 With Sectioned Folds" without sectioned folds.

The folding pattern still has the same problem as the RM. That is that 180 degrees valley folds are not possible with a thicker paper. Thus also for this design channels were added. Notice that some folds do not have channels, this is because adding a channel to these folds would only add a ring to the tube without any folds. Meaning that the expansion rate would suffer. The pattern that is seen in Fig X is the final pattern used in the final design.

4.4 Material

Defining the material used also largely determines the method of production and vice versa. So in this subsection the focus will lie on the production process's explored and the material possibilities that came with it.

Every module will require three type of parts: hinges, magnets and panels. For the magnets small cylindrical neodynium magnets were bought and attached to or inserted in the panels. The production of the hinges and the panels was less straightforward.

The first production process explored was 3d printing. The idea was that the printer could, using living hinges, make the origami structure out of one solid piece. By adding more material the 3d printer could make certain sections more stiff than others, creating living hinges. It would also allow the production process to work on a much smaller scale, as only a higher-grade 3d printer would be required. Although 3D printers can operate at nano scale [44] [62]. The printer most accesible during this thesis were Ultimaker, and Bambu Lab A1 mini with a nozzle of 0.4mm, which makes the minimum line width approximately 0.24mm [5] [3] which was verified during the production tests of this thesis. This ment that to print the living hignes the tesselation needed to be scaled up. Requiring every tile of the waterbomb to be 5cm by 5cm. This method would lead to a giant prototype, but still several tesselations with different living hinges were produced, however the hinges felt stiff and brittle. After opening and closing the prototype a few times, the first signs of material fatigue could already be seen. So from this point, there were two options. First one is start optimising the material and production process for small scale 3d printing. However, investing a lot of time and resources into doing that research, without knowing if the origami patterns would work in practice is risky. But to verify if the origami pattern works a prototype needs to be made. So instead of doing further research in optimising 3D printing different production methods were explored.

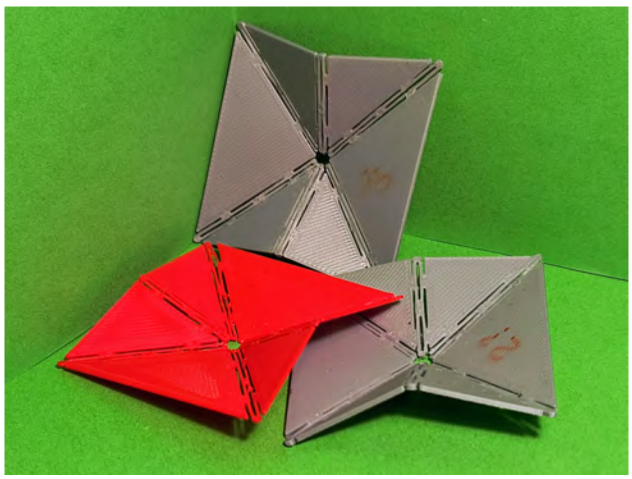

Figure 23: 3D printed prototypes of the waterbomb tesselation using living hinges

2 methods were explored in parallel. The first used rigid panels which were held in place by a mould, then a flexible resin is poured into the mould. When the resin has dried and the prototype removed from the mold the prototype the device is ready. To get a feel for the process the production method was tried out for a single waterbomb tile, using 3d printed parts and hot glue. The mold, ejector and prototype can be seen in Fig 24. Although the joints were much too stiff it showed the potential of this production process. There are a lot of different types of epoxy, however finding one that would stick to the panels and was flexible enough was difficult.

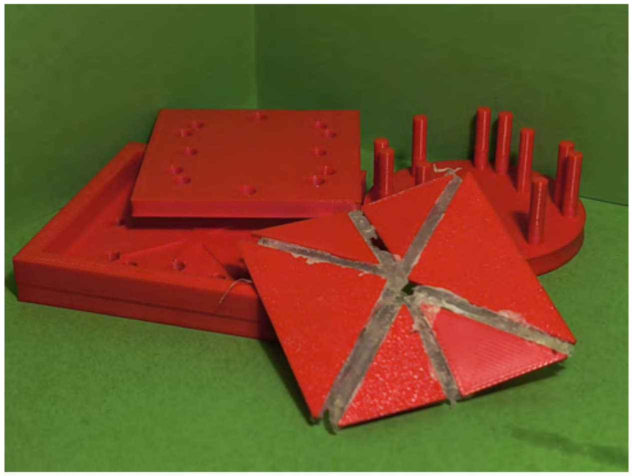

Figure 24: Mould, ejector, and prototype made during this thesis

The second method researched starts the same, with rigid panels being held in place by a mold. However instead of pouring resin, the panels are coated with a bit on the exposed side. Then a sheet of flexible material is placed on top these panels. As 3D printers were very accessible the material of the panels was chosen to be PLA. For the sheet a biocompatible soft plastic would be ideal. The most common material would be Polypropylene (PP) or Polyethylene (PE). However due to its low energy and difficult to penetrate surface glues have a difficulty bonding to these two materials [15] [13] [11]. As no glue in non-specialised hard-ware stores could provide a glue which sticked properly to the PP or PE, a different solution needed to be found. A method considered was using clear packing tape. These tapes are made of PP and already come with glue. However, prototyping the waterbomb pattern showed that this glue did not attach well to the panels. This can be seen in the bottom right of Fig 25. The panels displace when the pattern is folded even when both sides are taped.

Figure 25: Unfolded waterbomb prototype, made by using clear packaging tape and PLA panels.

The next material considered was PEEK, but before a prototype was made with that material, the question what is the goal of this prototype? Was once again asked. The goal of this prototype is to determine wheter these origami structures interacting with each other could lead to a locomotion. So biocompatibility is not yet necessary. Thus instead of a PEEK sheet, the much more available paper was used.

Paper is more stiff than plastic foil and two methods of reducing this stiffness were identified. First is using thinner paper, to test this three different thicknesses of paper were used, standard A4 printer paper which is 80 grams/meter^2 (gsm), thin printer paper of 50 gsm, transparant paper of 42 gsm, and 200H carbon paper with a weight of 28 gsm. During testing the thin paper and printer paper were able to maintain their structural integrity however transparant paper and carbon paper had too little stiffness to counteract the magnetic attraction between magnets and would collapse once the panels and magnets had been placed. For all papers "Loctide Super Glue-3" worked without any problems to attach the PLA panels to the paper.

The other method of reducing the stifness of the paper was to reduce the thickness of the paper only at the hinges. By engraving the joints using a laser cutter, paper is removed at the desired locations. To engrave paper the laser cutter must engrave at the perfect speed and laser power. If the speed is too low or the laser to intense a cut is created, if speed is too high or the laser intensity too low the engraving is not significant enough.

So for both 80 gsm and 50 gsm paper, an experiment was done with the goal to find the ideal combination of speed and power. This was done by asking the laser cutter to cut a line at different intensities and power. The test setup can be found in Appendix 9.2. The lines were judged on how well it engraved the paper. A scan of all lines can be found in Appendix 9.3. The resulting grades can be found in Appendix 9.3.3.

From these experiments came several settings that could be used. Such as a power percentage of 6 and speed of 5 for both paper thicknesses. However the most interesting was the unintended result of perforation. This happens because the laser blinks at a constant frequency, if the speed is high enough the location of the blink is always at a different location. And if the laser is powerful enough to perforate the paper during one such blink a perforation is created.

This perforation is more reliable with deviations in paper level but is also quicker. Increasing or decreasing flexibility is also easier as doubling the speed cuts the number of perforations in half. So perforation was the method chosen to create flexibility in paper. The perforation however made the the prototypes more fragile, the 50 gsm paper was difficult to assemble without tearing so 80 gsm paper was chosen as the final material. After informal testing, the best perforation was seen with a power percentage of 17% and speed of 10. Cutting was done with the same power just at a speed of 2.5

After perforation, the laser-cutter cut the outside lines of the pattern. On the resulting sheet the panels were glued manually at the desired location using a stencil, the panels had holes such that the magnets were placed at the correct position. A picture of this process can be seen in Fig 26.After that, when the glue dried, RM module was folded into the its desired shape.

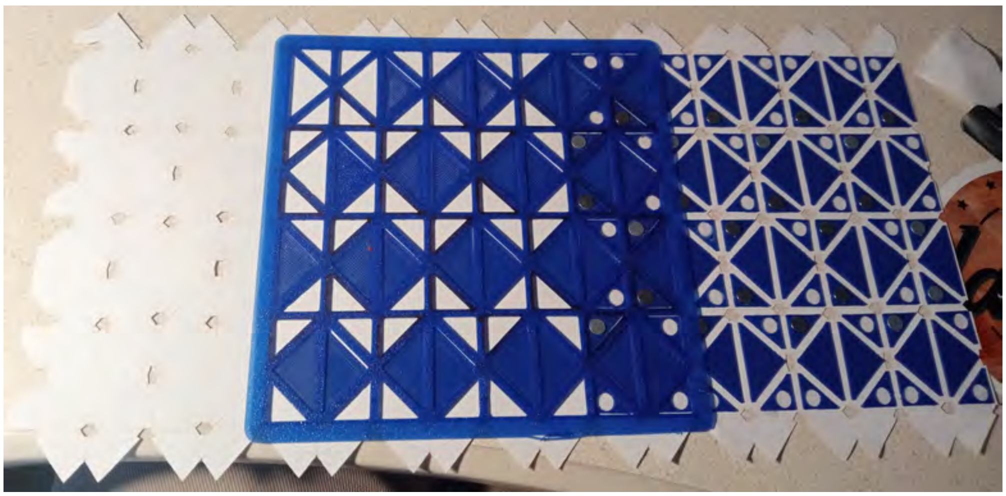

Figure 26: Assembly of an RM prototype, using a stencil to place the panels at the desired location

In conclusion, after careful consideration, the best production method to create the prototypes is by first perforating the hinges onto a standard 80 gsm paper using a laser cutter, and are the outside lines cut. Then using Loctide Super glue-3, the PLA 3D-printed panels are glued on top of the paper, together with the magnets, using a stencil. The entire system is manually folded and glued into a tube, and the prototype is manufactured.

4.5 Magnet placement

Now that the production method and materials are clear. It should now be determined what the exact magnet placement is going to be. Before going to a specific origami pattern it is important to consider the relationship between the number of possible magnets and the spring stiffness of the joints. If magnets are placed close to each other, they will attract each other. The spring stiffness of the joints normally prevents this from happening. However if during any folding configuration, the magnets get too close to each other, will lead to a collapse. If that is not the case then adding more magnets will improve the expansion rate and speed, as will be explained in chapter 6, which are desired properties. So as many magnets need to be placed as possible, without the magnets attracting each other with a force higher than created by the spring stiffness of the joints.

4.5.1 Magnet placement for RM-module

To determine the optimal magnet placement, first, the question was asked: What would the magnets be placed if there were no repercussions for having too many magnets? Also, the assumption was made that every panel can be transformed into a dipole magnet in any direction. To keep up the radial symmetry, every tile of the RM would have the exact same magnet setup, this simplifies the search for the optimal setup as only one tile can be considered.

In previous research, a Matlab model was used to simulate the behaviour of origami structures with magnetic panels inside uniform magnetic fields [56]. This model has a downside in that it can only model small-scale structures such as single or double tesselations. But as only one tesselation needs to be simulated for this experiment this script was used to find the optimal magnet placements.

The important inputs of the model are as follows: Origami pattern including folding direction, initial displacement, magnetic strength vector of each panel, magnetic field vector of the uniform magnetic field, DOF for every node, and spring stiffness of the joints. The output is the angle relative to the magnetic field of all panels when the spring stiffness and the magnetic torque are in equilibrium.

Using this script, the optimal magnet direction would be decided. To do this four magnet tesselation configurations were run through the model. All configurations had the goal to retract as much as possible from an already slightly contracted position. With the only difference between configurations being the direction of the magnetic fields created by the panels. The setup before applying any magnetic field can be seen in Fig 27a. To determine how much the structure has retracted, the angle between panel 1 and 6 is used as parameter. As panel 1 is locked at 0 degrees, which can be seen in Fig 27e, the angle between panel 1 and 6, will be refered to as the retraction index and can be calculated as follows $180 -$ angle panel six. So a smaller retraction index means more retraction.

First configuration was the base-line test. This configuration of the waterbomb came with the script and can be seen in Fig 27a and was proven to work. This configuration was also used to determine the initial inputs, such as stifness and magnetic strength. With a retraction index of 145.2°, this configuration sets a strong baseline.

A problem with this configuration is however that the magnetic field comes from the wrong direction, looking at an image of the waterbomb prototype such as Fig x. It is clear the the current magntic field is not in line with the symmetry axis. Thus configuration 2, which can be seen in Fig 27b, changes nothing else but aligns the magnetic field along the symmetry axis. The result is a confused tile trying to rotate, which can be seen in Fig 27f.

The following configuration was the one that had been in mind during the initial development stages of the prototype. The magnets instead of pointing out of the paper, are placed in line with the paper, and the magnet on panel 6 is removed, see Fig 27c. This leads to a retraction index of 167.25°, this can be seen in Fig 27g.

The last configuration can be seen in Fix 27d, here the magnets are pointing out the paper. Which leads to an even better result with a retraction index of 166.07°. This result can be seen in Fig 27h.

All retraction indexes are summarised in Tab 3. It is not suprising that the base configuration has the best retraction index, as it has an extra magnet on panel 6. However the magnetic field being in the wrong direction means that this configuration can not be used. In second comes configuration 4, so that is the configuration that will be used as baseline. Configuration c & d receive the exact same forces but inversed. If the focus is on retraction then 3 is ideal while if the focus is on extension then 4 is more ideal.

Table 3: Retraction index of the different magnet placement configurations for the RM module

Setup	Retraction index
(a)	145.2
(b)	-
(c)	167.2
(d)	166.07

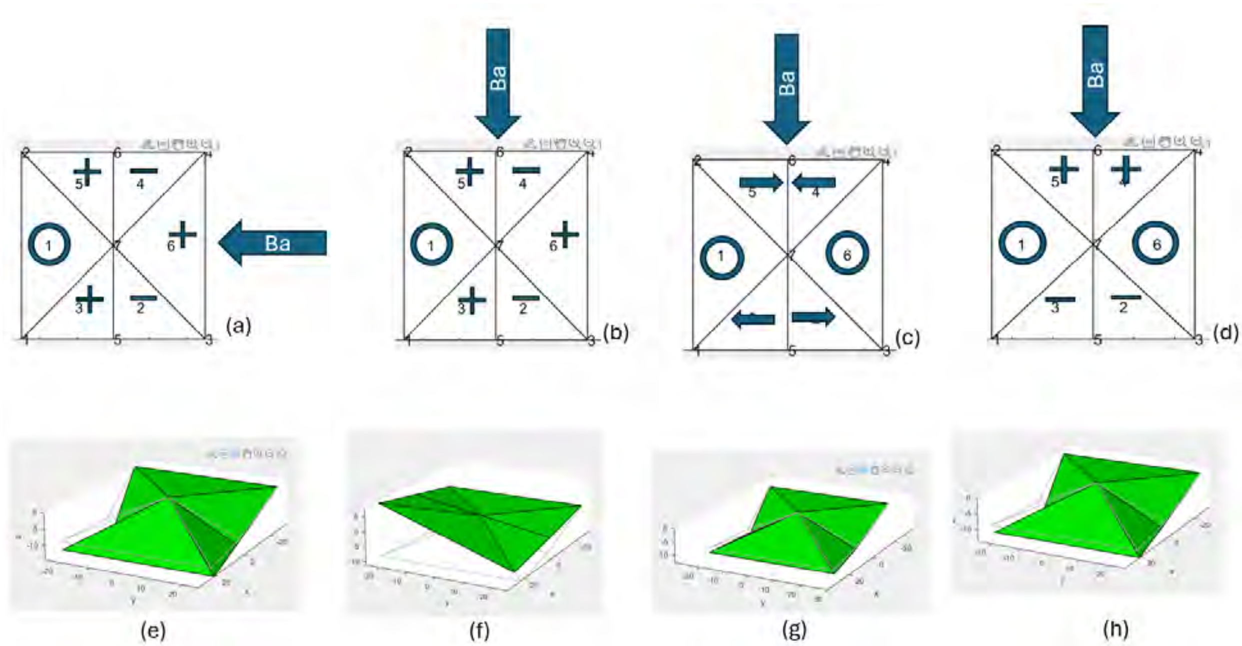

Figure 27: Magnet placement and its resulting simulated behaviour

Reality is however that placing a magnet on all tiles as implied by these tests will result in the magnets stacking onto each other. After testing out different configurations, a configuration was found which allowed for 50% of the desired planes has a magnet. See Fig x the outer planes do not have a magnet as these planes are static. This configuration makes sure that when collapsed always four planes are between every magnet, this prevents the magnets from staying at a distance and thus have a low magnetic attraction to oneanother. This configuration also does not reduce the axial symmetry.

4.5.2 Magnet placement for AXM-module

Deciding the ideal magnetic placement of the magnetic direction for the AXM was more straightforward. Two configurations were tested, with the difference being that the first configuration has the magnets pointing out of the paper while the second has the magnets in line. with the paper, the schematics can be seen in Fig Xa and Xb.

Node 3 and 8 are locked. The retraction index is calculated as the angle between panel 1 and 3, the results can again be seen in table x. Configuration 1 is the clear winner so this configuration was chosen.

Placing the magnets in reality was difficult, the first try can be seen in Fig x. Only 25% of the panels which could have a magnet as the rule of four segments between every magnet from the waterbomb was used. To increase expansionrate a magnet configuration with double the magnets can be seen in Fig x. This configuration however collapsed immediately, see Fig x. So the initial configuration was used in the final prototype

4.5.3 Improvements

There are some things that could be studied further in later research. As currently only magnets which magnetic field were perpendicular or in line with the paper are considered, as these are easily commercially available. Having the magnets be at an offset angle of the plane it is resting on might lead to more efficient or stable results. Although most likely it will only displace the expansion region. So instead of expanding from 20% to 60% it might expand from 40% to 80%.

5 Prototype experiments

With the design of the prototype set it stone the next step was to test it to prove that the concept would work. This is done in three sets of experiments. The first set explores the behaviour of the modules separately in a slowly changing magnetic field. This will provide insight in the folding behaviour, the expansion, and potential history being present. The second experiment will put every module separately in a quickly changing field. This is done to collect the prototypes expansionspeed and valuable parameters for the model developed in chapter 6.The last experiment will be an integration test with all three modules connected to each other being placed inside a tube. The magnetic field will be alternating as described in chapter 4.1 Locomotion. At the end of every experiments the results will immediatly be shown and discussed.

5.1 Setup

The test setup can be seen in Fig 28. Its basis is the PACMAG, which using only its X-axis coils creates a magnetic field. The maximum field strength that can be generated is 50 mT in two directions, so the range of the magnetic field is 50 to -50 mT. Inside this magnetic field the module is placed along a glass rod. A camera from above captured a frame every 500 ms for 10 cycles. The resulting video was then used to track the radial expansion of the RM. And the axial expansion was tracked for the AXM. The software used to track this was "Tracker - Video Analysis and Modeling Tool" [12].

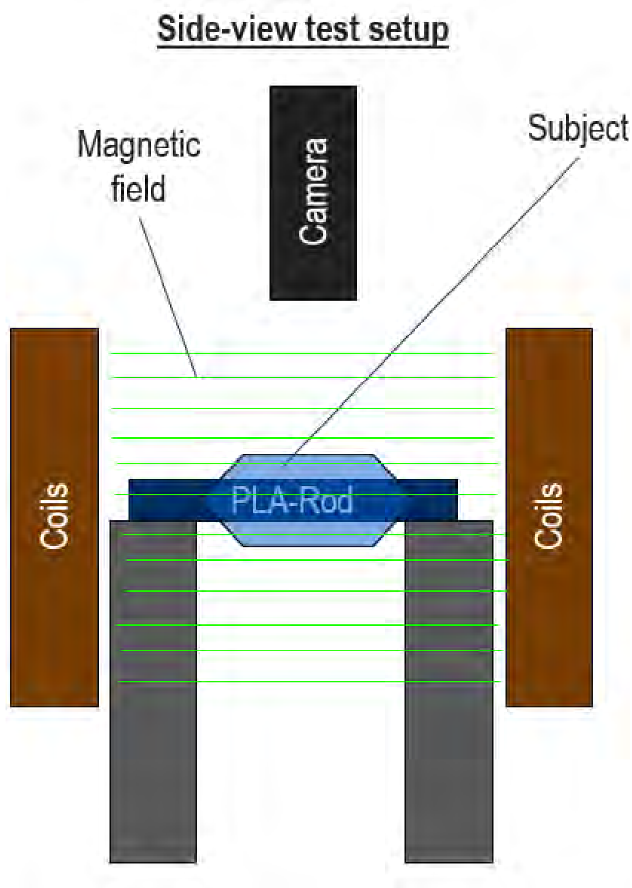

Figure 28: Sketch of setup used during the waterbomb experiment

5.2 Slow wave input

As mentioned in the intro the goal of this experiment is to gain insight in the folding behaviour of the modules and know the expansion rate. As input was thus a slowly rising magnetic field used. This field slowly alternated between 50 mT and -50 mT in a sinuswave with a cycle time of 20.000 ms. Such a long cycle means that momentum is negligble in the results and thus alle behaviour is purely from the geometry of the origami and its interaction with the magnets.

The resulting expansion of both the RM and the AXM can be found in the Fig 29.

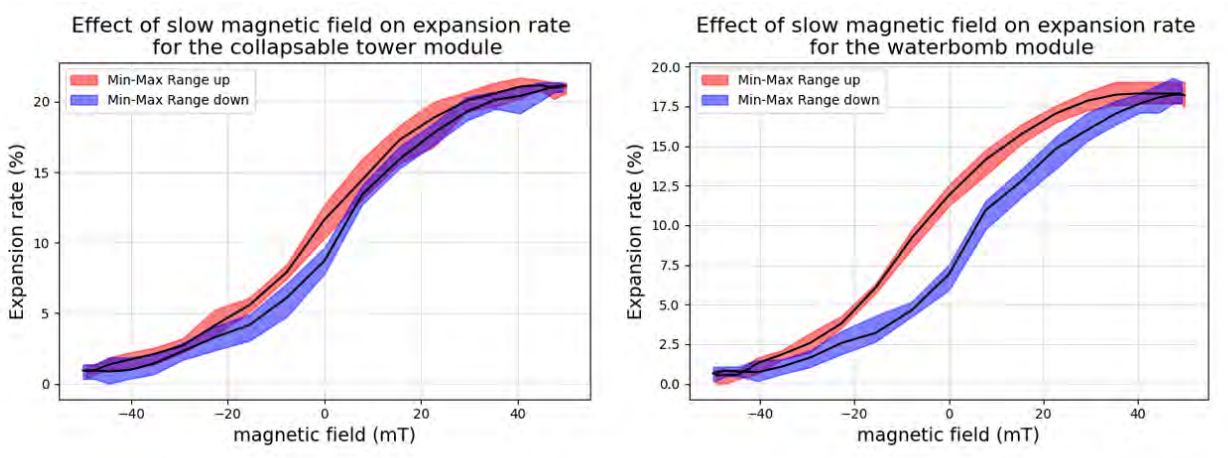

Figure 29: Results of the slow changing field experiment for both the AXM and RM module

The graph shows the expansion rate of the module over the magnetic field. It consists of two parts: red, showing the expansion rate for different magnetic fields when the waterbomb is expanding. And blue, showing the expansion rate at different magnetic fields when the waterbomb is retracting. The black line is the mean while the colored area is the area between the maximum and minimum expansion rate for that magnetic field.

The first thing to notice is the S-shape of all the curves, this shows that going from zero to ten mT creates a larger displacement than going from 40 to 50. This makes sense as the spring stifness increases linearly while the magnetic torque increases along a sinuswave, for why see chapter 6 Modeling.

The second thing to notice is that especially the RM seems to have the behaviour that it matters whether or not the module was just expanded or retracted. For example, the expansion rate when the field is off (so 0 mT) is 12% when coming from a total retraction, while the expansion rate is 7% when coming from total expansion. This is counter intuitive, as a baseline resistence would explain the opposite behaviour. The hypothesis is that a mistake has been made during the production of the plots that results in the expanding and retracting data to be swapped. Meaning retraction is actually expansion and vice versa. After double checking no mistakes were found in the plotting program, so the reason remains unknown.

But the most important of this graph is that the maximum expansion rate of the prototype can be read. For the RM this seems to be 17% where for the AXM it is 20%.

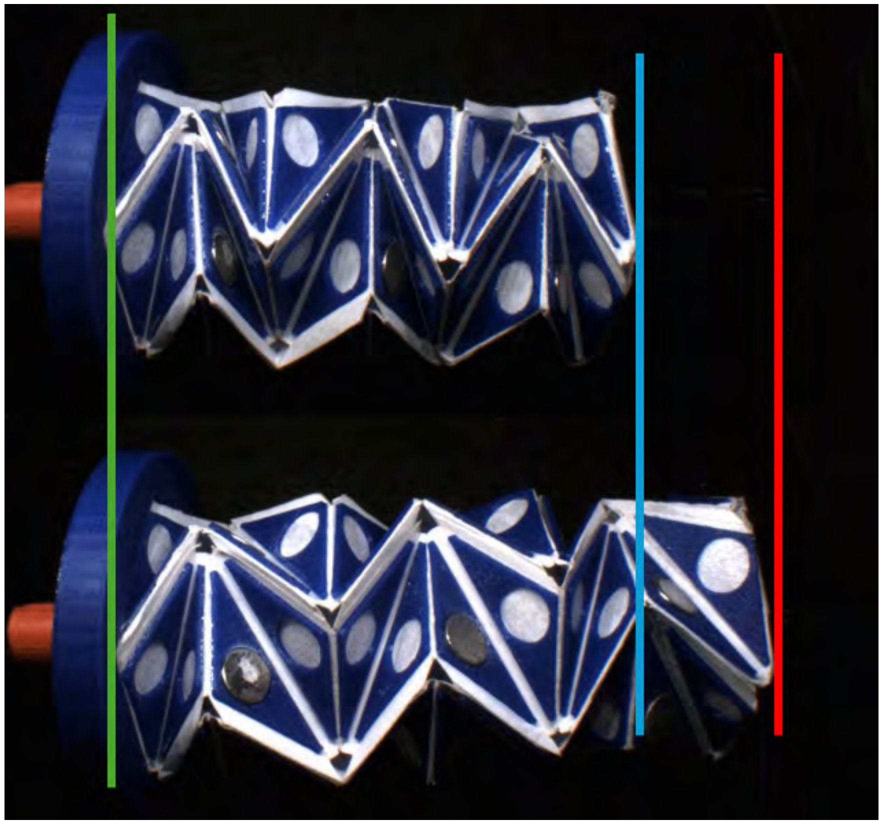

Figure 30: Frames of AXM module being both collapsed and exanded during the slow wave input experiment. Green: Baseline, Blue:maximum retraction,Red:maximum expansion

Figure 31: Frames of RM module being both collapsed and exanded during the slow wave input experiment. Green: Baseline, Blue:maximum retraction,Red:maximum expansion

5.3 Puls input

The following experiment had as goal to determine the expansion speed of the modules and gain more insight in the behaviour of the modules for the model in chapter 6. The settling time was determined by measuring when the average of all cycles reach 95% expansion. Retracting time was determined by the time it takes the average to reach 5%. As the system has to stabilise, the latest point that the 95% or 5% line is crossed is measured.

For this test, the same setup was used as with the Slow wave experiment. The only two changes are that the magnetic field now instantly switches from -50 mT to 50 mT and vice versa every second. The other

Table 4: Settling times of RM and AXM.

Module	Time to 95% (ms)	Time to 5% (ms)
RM	505	420
AXM	201	195
Δ	304	225

change is that the camera now captures at every 0.022 ms, better known as 45 frames per second.

The graphs of the RM and AXM can be found in Fig 32a b respectively. The time it takes for the modules to reach the 95% and 5% mark can be found in Table 4.

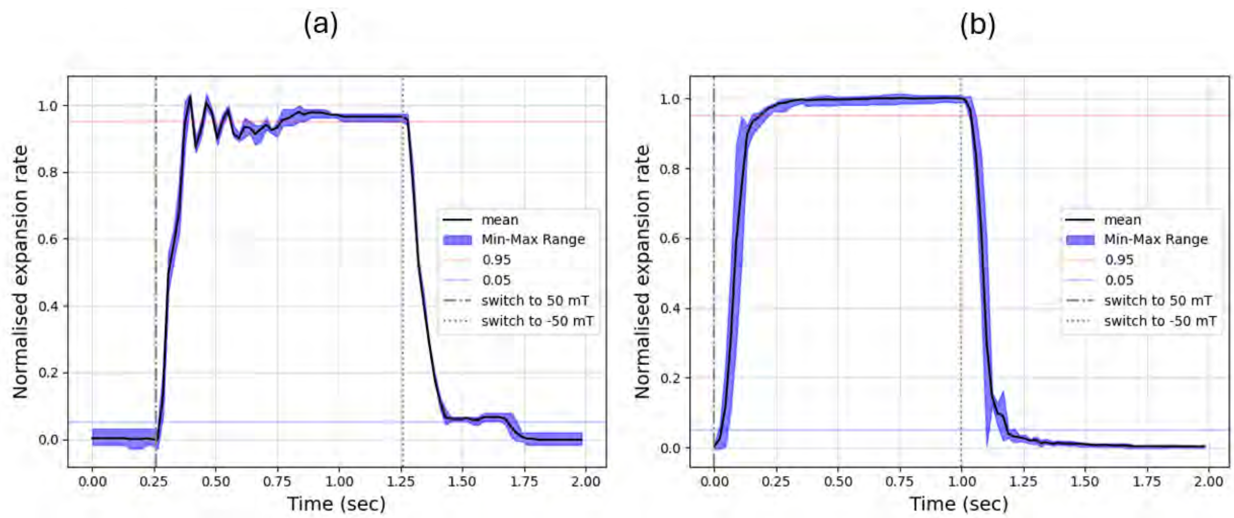

Figure 32: Average normalised expansion rate over four cycles for (a): the RM. And (b) the AXM

The results of the AXM gives a good insight in the behaviour of this module. However the expansion and retraction time is currently much lower than that of the RM. In reality this module will take longer as the AXM needs to displace the RM, and thus has more momentum. This is further explored in chapter 6.

5.4 Integration test

The last test done in this thesis was the integration test, the goal is to find out if the modules interact with each other in the expected way.

The 3 modules were connected to each using glue, where the second waterbomb is a mirror of the first. This system was placed inside a PVC tube with a diameter of x mm's. This tube thickness was chosen as this seemed to be the optimal thickness for the waterbomb to work. A glass shaft ran through the centre of the PVC pipe to simulate the system floating inside the aorta. A sketch of the setup can be found in Fig X. The PACMAG was instructed to switch between 50 and -50 mT every 500ms. The centre of mass of all three modules was tracked using the Tracker software. The displacement of the modules was then plotted per cycle over time and can be seen in Fig x.

Figure of setup

Graph of displacement of each module per cycle over time

Snapshots of device moving

In this part of this subsection the results are discussed a conclusion is drawn.

5.5 Discussion

During the experiments with the collapsable tower the module tried to rotate its symmetry axis such that the same side always faced the positive side of the magnetic field. It is intuitive to think that this is an expected behaviour, however in this section it will be explained why in a perfect world this should not happen but that due to imperfections during the production process this phenomenon does occurs.

Take a rod with two magnets on top such as in Fig x. When placed under a magnetic field both magnets want to rotate to allign, however because the system is symmetric the moments that are created by the magnets cancel each other out. Thus the rod does not move. Now change the angle of one of the magnets slighlty such as in Fig x. If under this condition a magnetic field is applied. The momentum created by the magnets is different. Resulting in momentums not canceling each other out. What leads to a small remaining momentum rotating the rod.

This is also what happens in the collapsable tower, but then in 3 dimensions. All magnets try to rotate the collapsable tower in their direction however their netto momentum is theoretically 0. Human error most likely caused the joints to not be the exact same stiffness what causes some magnets to sometimes be at different angles than others. Leading to different moments and thus a non-zero remaining moment on the system.

But if that happens to the collapsable tower, then why does that not happen to the waterbomb? This is because of two reasons, the first is that the parts are more geometrically locked. Meaning that when one magnet rotates others are geometrically forced to move too. Also as the number of magnets is higher and their size is smaller, it reduces the influence of one magnet on the total momentum. If only one magnet differs in created moment then the netto moment is low.

6 Mass-spring-damper model

To improve the parameters of the prototype a model needs to be made to simulate the behaviour of the entire modules inside a magnetic field. Previously in this thesis, a model made by Sam Tijhuis was used to simulate the behaviour of the modules. This model can not be reused for two reasons. The first reason is that this model focuses on individual tiles in small scale, full 4x8 tesselations patterns are not possible, thus the assumption must be made that all tiles behave the same and do not significantly interact with each other. But even if a strong enough computer can be found The second reason is that both RM and collapsable tower need to be folded from a tube of paper, not a flat piece of paper. This adjustment is not possible in the Sam's current model. The solution to both problems is to either, upgrade the model to use more tesselations and give the program the ability to fold paper tubes instead of flat pieces of paper or develop a new model focussing on the behaviour of the module in its entirety. During the production of the prototypes of the modules, it was noticed how the module behaved similarly to a Mass-spring-damper model, thus in this chapter a model of the module expansionrate based on the MSD model is proposed.

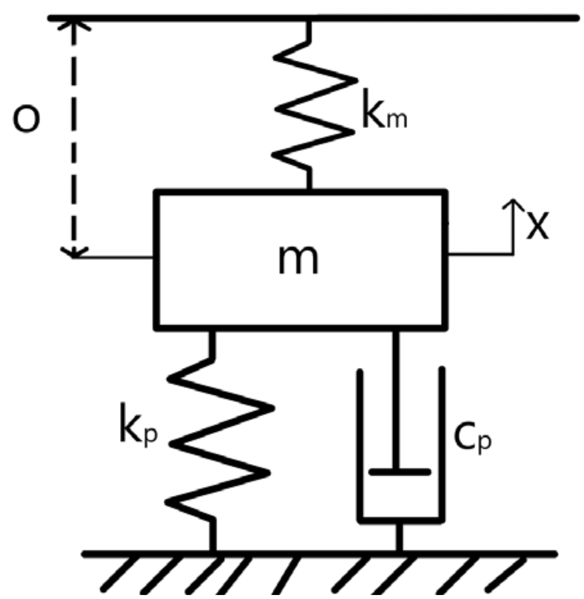

Figure 33: Altered MSD model used in this thesis for simulating the indidivual behaviour of the modules

6.1 Creating the model

To start, a module (does not matter which) is seen as a black box. The input of this box is the force created by the magnets inside the magnetic field, the output would be the expansion of the module. A model to fit the black box would be the 1 Degree of Freedom (DOF) Mass-Spring-Damper Model (MSDM). Force F can be defined as being linearly proportional to the torque created by the magnets inside the magnetic field, so $\tau = F_m * n$ where tau is the torque created by the magnets, F_m is the force inside the model and n is a constant. Following that, to fully fit the model inside the black box, the assumption is made that the displacement x is linearly proportional to the expansion percentage of the module, so $x = \text{expansion percentage} * n$ where n is once again a constant. A visualisation of this model can be seen in Fig 33

Now that this model fits the black box, the equation of motion can be derived

$$\sum F = ma \tag{3}$$

$$\sum F = m\ddot{x} \tag{4}$$

Then insert the force created by the spring and the damper and the external force F_m.

$$F_m - kx - c\dot{x} = m\ddot{x} \tag{5}$$

Table 5: Parameters used in the MSD model and its real life counterparts

Model	Real module
x	Current expansion percentage
o	Geometric maximum expansion percentage
m	Inertia and Mass
k_p	Stiffness of the creases
k_m	Coefficient for magnetic power (nr of magnets, magnetic field strength)
C_p	Coefficient for energy loss (friction, deformation)

Table 6: Parameter values used in simulation

Variable	RM expanding	RM decreasing	AXM expanding	AXM decreasing
o	250	TBD	TBD	TBD
m	0.01	TBD	TBD	TBD
kp	3.75	TBD	TBD	TBD
km	26.25	TBD	TBD	TBD
cp	0.19	TBD	TBD	TBD

Now before doing any calculations, F_m needs to be adressed. This force is not constant as in chapter 2.8. But should be seen as a non-linear spring. The torque created by the magnets can be calculated using $\tau = M \times B$. As the error between the magnets and magnetic field direction decreases the torque created decreases as well, along a sinus curve. The reason that the torque is proportional to the error along a sinuswave is because the cross product formula can also be written as

$$\tau = |M||B|\sin(\theta) \tag{6}$$

Where theta is the difference in angle between the dipole magnets and the magnetic field. So inserting $F_m = \tau$ to this formula creates $F_m = |M||B|\sin(\theta)n$. Knowing that $F_m = 0$ during a total collapse and when the module is totally open, means that when x is equal to the geometric maximum expansion percentage or equal to the geometric minimum expansion percentage than Fm is 0. Assuming x=0 lies in the middle, then $\sin(\theta)$ can be rewritten as $\cos(\pi\frac{x}{o})$. That only leaves the parameters $|M|$, $|B|$, and n. These variables Magnetic dipole, field strength, and constant n are all constant in our simulation and are summarised as value k_m This resulted in the following equations of motion.

$$F_m - kx - c\dot{x} = m\ddot{x} \tag{7}$$

$$m\ddot{x} + k_p x + c_p\dot{x} - k_m(\cos(\pi\frac{x}{o})) = 0 \tag{8}$$

The translation from model parameter to real life parameter is summarised in Table 5 and is as follows: Reducing mass in the model (m) is the same as reducing mass and or inertia in the module. Reducing the k_p is making the creases of the paper less stiff. Reducing damping reduces the main losses of energy in the system: friction, and material deformation. Increasing k_m increases the magnetic field, the number of magnets in the module or, the strength of the magnets.

6.2 Finding the correct parameters

Now that a model has been created the correct parameter values need to be found. This was done by making the model simulate the experiment of the quickly changing field found in chapter 5.3. A blind guess was made for the parameters and the resulting behaviour was compared to the results from the real-life experiment. Then adjustments were made to the parameters and the behaviour was compared again. This continued until the behaviour was close enough to reality. The result of the final configuration compared to reality can be found in Fig 34. The parameters used in this configuration can be found in table 6.

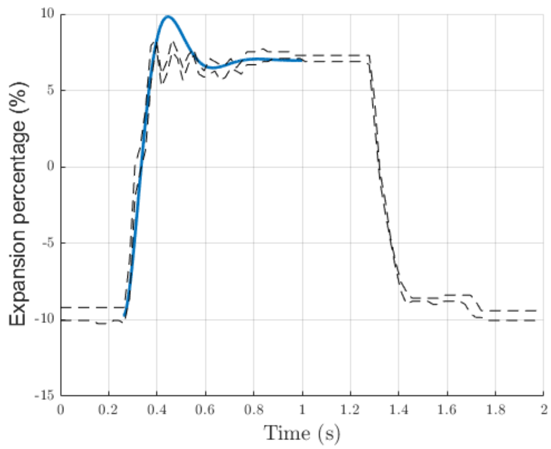

Figure 34: Graph visualising difference between model and reality. Blue: Simulation. Black-dashed: Max and Min values of prototype during experiment.

6.3 Using the model to find prototype improvements

Now that the model has the correct parameters to simulate the prototype, the parameters can be adjusted to see the impact

6.3.1 RM expansionrate

The expansion rate of the simulation is fully determined by the ratio between k_p and k_m. Increasing k_m while reducing k_p increases the expansionrate. In cases where k_m and k_p are close in value, the expansionrate can be approximated with the following formula expansionrate $= 2\frac{k_m+1}{k_p}$. This formula stops being effective once k_m becomes much larger than k_p. As at a factor of 25 the simulated expansion rate is 46.0%, two entire percantage of the expected 48%. At a factor of 50 the expansionrate is 84% an entire 16% lower than expected. This reduction is because as x increase k_m reduces in effectivity while k_p is modeled as a linear spring and behaves similar at all expansion percentages.

The expansion rate requirement was set at 19%, this means an expansion from zero of ±8.5%. To achieve this expansion percentage the ratio between k_m and k_p needs to be at least 8.5 to 1. The ratio of the current prototype is 7 to 1, see Fig **??**. So to fulfill the requirement of 19% expansion either the paper needs to reduce its stiffness with a factor of 1.19, or the magnetic interaction needs to increase by a factor of 1.19. Either by adding stronger magnets or increasing the field to 60mT. Although the field can not increase its magnetic field, reducing the crease stiffness or increasing the magnetic strength by a factor of 1.19 should be possible.

That all being said, the expansion target in the requirements was set at 100%, the correct ratio for this expansionrate of k_m and k_p was found to be 64 to 1. This leads to an expansionrate of 100.0%, as can be seen in Fig **??**. This means that in order for the prototype to reach at least an expansion rate of 100% either the crease stiffness needs to decrease by a factor of 9.2. Or the magnetic interaction needs to increase by a factor of 9.2. As placing 10 times more magnets, or increasing the magnetic field to 460mT is not possible, the best plan of action would be to reduce the stiffness of the creases. Perforating the paper more often or using a material 9.2 times less stiff than paper are two potential solutions that could lead to the desired expansionrate of 100%.

6.3.2 AXM speed

*Needs to be written

6.4 Shortcomings of the model

The MDSM model is not flawless relative to the model by Sam. In the MDS model certain individual real life parameters are more difficult to link to virtual ones. For example when a paper joint is folded with more force the zero point of the zero point of the spring is set to a different angle. This is a simple adjustment in Sam's model. In the MDSM various variables all need to be adjusted x_e, k_m, and k_p to change this one parameter.

6.5 Conclusion

Although this model is not perfect it provides insight in the effects of changing certain parameters of both the RM as the AXM. The resting expansion value is proportional to the k_m/k_p. Decreasing k_p of the current RM prototype by a factor of 50 is needed in order for the RM to fulfill its goal expanion of 100%. The reaction speed of the system is controlled by all factors. A reduction in mass,kp, and damping reduces the reaction speed. The same effect happens when increasing km or o. The best method to reduce the speed of the AXM is by xxx.

Table 7: Evaluation of all requirements based on final prototype

	Requirement	Was requirement met?
R1	Outer diameter adaptability	No
R2	Aortic wall safety	needs to be tested
R3	Locomotion	TBD
R4	Continued blood flow	needs to be tested
R5	Failure rate	needs to be tested
R6	Biocompatability	No
R7	Simplicity	No
R8	Origami Engineering	Yes
R9	Magnetic Actuation	Yes
rm-R1	Radial expansion	No
rm-R2	No axial expansion	Yes
rm-R3	Module interface	Yes
rm-R4	Field along symmetry axis	Yes
rm-R5	Quick expansion	TBD
axm-R1	Axial expansion	Yes
axm-R2	No radial expansion	Yes
axm-R3	Module interface	Yes
axm-R4	Field along symmetry axis	Yes
axm-R5	Slow expansion	TBD

7 Evaluation and discussion

In this chapter the final design and prototype will be weight against the requirements set during the Preliminary design in chapter 3.1 and the additional requirements set in chapter 4.2. The evaluation is summarised in Table 7. Explanations and recommended adjustments will be given for the requirements that were not or only partly met. At the end of this chapter potential use cases are explored. .

7.1 Requirements met

R8 Origami Engineering The device consists entirely out of origami structures, thus the requirement use origami engineering has been met.

R9 Magnetic actuation The device does move under magnetic field, although for the waterbombs not as much as desired this requirement has been met.

w-R2 No axial expansion The origami design chosen for the waterbomb has no axial expansion. This requirement has been met.

w-R3 Module interface The origami design chosen for the waterbomb has a static interface that connects nicely to the collapsable tower module, as proven in the integration test. This requirement has been met.

w-R4 Field along symmetry axis The origami design keep the symmetry axis in line with the field. The magnet placement does not reduce the number of symmetry arm, so the number of symmetry arms is 9. Which is a nice and high number. This requirement has been met.

c-R1 Axial expansion The collapsable tower has an axial expansion of just above 20% although the initial goal of 100% expansion was not met. The 20% expansion should be enough. Just more cycles are needed for the displacement of the device. This requirement has been met.

7.2 Requirements not met

R1 Outer diameter adaptability Safely to say the requirement stating that the outer diameter needs to be 31.44mm and can adjust is outer diameter by 8% both inwards and outward, was not met. The waterbomb decides the devices outer diameter and has in resting state a diameter of 64mm, which is twice as large as it should be. The device can adjust its diameter using a magnetic field with 8% inwards and outwards. The design, if more optimised should be easy to scale down, no electronics or devices with minimal sizes are used, so the system should work even in micro scale. Production at a smaller scale would benefit from a more simplistic design with fewer parts, how that is possible is explained under the evaluation of the requirement.

R6 biocompatibility The materials chosen for the prototype were not selected for its biocompatibility. Printer-paper, Loctide glue (source) are not biocompatible. However PLA and neodymium are [29](source). Material is not the only thing deciding the biocompatibility as geometry, surface texture and coating also need to be taken into account. This was however not done as the requirement already failed on its basic materials and this was out of the scope of the project. So to meet this requirement the following needs to be done: Replace the paper and the glue with biocompatible alternatives and perform a biocompatibility study on the shape of this design.

R7 Simplicity This requirement has not been met as the device consists of a lot of components. The waterbomb has 36 tiles, with each tile having 6 plastic panels and 1.5 magnets, adding to that the paper brings the total to 271 parts for only the waterbomb. The collapsable tower has a similar problem. It has 30 tiles, with each tile containing 2 plastic panels and 0.5 magnets. Adding once again the piece of paper brings the total to 76 parts. The device consists however of two waterbombs and one collapsable tower, which brings the final number of parts used to produce this device to 618. This number is too high, to call the device simple so the requirement is not met. Reducing the number of parts is possible if the plastic panels can be integrated into the paper. By for example using much thicker paper but keeping the hinge stiffness similar. This would bring the number of parts down to 126, 123 magnets and 3 pieces of paper. Reducing the number of magnets is more difficult, changing the paper to a metal fiber filled resin and making certain panels magnetic could bring down the number of parts to only 3. A sketch of this can be found in Fig x

w-R1 Radial expansion The requirement set that the waterbomb should at least expand 19% with a target expansion of 100%. The current waterbomb prototype expands only 17% and thus does not fulfil the requirement and can not locomote inside a aorta which varies in diameter. The solution as mentioned in chapter 6 is to decrease the stiffness of the creases by a parameter1 and parameter2.

7.3 Requirements that need to be tested

R2 Aortic Wall Safety Although the design was made with aortic wall safety in mind. To test this requirement the design must be set in stone, as material choice and a different expansion rate will be of great influence of keeping the aorta undamaged. The recommendation is thus to first optimise the design by defining the material and expansion rate, taking aortic wall safety in mind. And only after that start physical tests to determine the Aortic Wall Safety of the device.

R4 Continued blood flow Again, the device was designed with allowing continued blood flow in mind. The device is hollow and blood should be able to pass through the device. However, this has not been tested virtually or practically during this thesis. As blood flow obstruction is defined by geometry, this can already be tested by virtually or physically measuring the pressure drop created by the prototype.

R5 Failure rate The current design consists of many hinges, as the material is yet undefined failure rate of the individual hinges is hard to determine. An initial failure mode analysis can be made. As the design of the device is still very flexible this method of identifying risks could benefit identifying key parameters that need to be changed.

7.4 Potential uses

The device was created to help with stent placement in the aorta however there are other use case scenarios that this device might aid. There are five systems identified in which the device could be proven to provide useful aid: The circulatory system, the respiratory system, the digestive system, the urinary system and the reproductive system. These will be discussed one by one.

The circulatory system is a given, the device was created to aid in AAA and thus designed to traverse arteries. Scaling down the system would also allow the device to traverse smaller arteries, or aid cardiovascular treatments. Robots to aid the movement of the guidewire are already in development and this device could be a good alternative [35].

For aiding the respiratory system the continued blood flow parameter really shines. With the potential ability to traverse the Windpipe without blocking air flow could be an interesting alternative to bronchoscopy.

For the digestive system capsule robots are already in development, as mentioned in the competitor analysis. This device would distinct itself from the competitors as it can traverse the digestive track without the use of the peristaltic movement of the bowels. Thus this device has more control.

For the urinary track the device, if scaled down enough, the device can be placed via the bladder inside the ureters or urethra to remove kidneystones which became stuck and otherwise would have required surgery.

It is tempting to scale up the size of the device and use it for traversing sewage. However, due to the system requiring a uniform magnetic field along its symmetry axis, the device can not be used for underground tube systems. As creating a uniform magnetic field from the outside of those underground tubes would require the tubes to be dug up. This would not be the case for above-ground tube networks. The magnetic field could be created by two coils around the tube in question. These tube networks could be inspected from the inside out without interrupting the liquid flow.

8 Conclusion

In this thesis a intravenous locomotion device has been designed. After ideation 3 concepts were developed from which one was chosen. This modular concept based on a worm was named the Modworm. The modules were first tested seperately to determine its parameters and then tested together inside a integration test. The results of these experiments led to the conclusion that several parameters such as expansion rate of the waterbomb and XXXX need to be improved. To ease with determining which change of the prototype would lead to better results, a MSD-model was made. The findings of the experiments and the msd model were then used to evaluate the requirements 19 requirements. 9 of the requirements were met, 3 are inconclusive and need to be tested and 4 requirements have not been met. To meet these requirements the Modworm needs to be scaled down to half its size, reduce its number of parts, increase the expansion rate of the waterbomb module, and replace the current materials with biomaterials. Further research needs to be done on Aortic wall safety, created pressure drop, and failure mode analysis. For potential uses outside the circulatory track the Modworm has a lot of potential in other bodily systems such as the digestive and urinary tracks.
In conclusion the Modworm is a device that has great potential but does not meet all its requirements yet. Meeting these requirements is however very possible with further research.

References

[1] Collapsible Paper Tower Helix Decagon - YouTube.

[2] Collapsible Tower Dodecagon V2 With Sectioned Folds - YouTube.

[3] Help With 0.2 MM Nozzle - Improve your 3D prints - UltiMaker Community of 3D Printing Experts.

[4] Houten bouwpakketten en modelbouw — Robotime Nederland.

[5] How thin can a 3D printer print? — dddrop - Professional FFF 3D Printers - Additive manufacturing.

[6] How To Make an Origami Flapping Bird - EASY step by step! - YouTube.

[7] Japanese Hobbies: CPs - The Crane.

[8] Origami - Japanese Art, Paper Folding, History — Britannica.

[9] Origami Simulator.

[10] Robotime Electric Guitar — Houten 3D DIY bouwset electrische gitaar — Robotime Nederland.

[11] The Best Polyethylene & Polypropylene Glues — Bonding PP & PE Plastic.

[12] Tracker Video Analysis and Modeling Tool for Physics Education.

[13] Why Polypropylene is so difficult to Bond ? - Adhesives & sealants engineering — Eng-Tips.

[14] Mohammad AL-Rawi, Ahmed M. AL-Jumaily, and Djelloul Belkacemi. Non-invasive diagnostics of blockage growth in the descending aorta-computational approach. *Medical & Biological Engineering & Computing*, 60(11):3265–3279, 11 2022.

[15] Besley Thomas. Bonding polypropylene with glue: Best methods and tips - Forgeway Ltd.

[16] Jared T. Bruton, Todd G. Nelson, Trent K. Zimmerman, Janette D. Fernelius, Spencer P. Magleby, and Larry L. Howell. Packing and deploying Soft Origami to and from cylindrical volumes with application to automotive airbags. *Royal Society Open Science*, 3(9), 9 2016.

[17] Ian Chaston. Technological Entrepreneurship: Technology-Driven vs Market-Driven Innovation. *Technological Entrepreneurship: Technology-Driven vs Market-Driven Innovation*, pages 1–299, 1 2017.

[18] Bogdan Ciszek, Krzysztof Cieślicki, Paweł Krajewski, and Stefan K. Piechnik. Critical Pressure for Arterial Wall Rupture in Major Human Cerebral Arteries. *Stroke*, 44(11):3226–3228, 11 2013.

[19] Gastone Ciuti, R Caliò, D Camboni, L Neri, F Bianchi, A Arezzo, A Koulaouzidis, S Schostek, D Stoyanov, C M Oddo, B Magnani, A Menciassi, M Morino, M O Schurr, and P Dario. Frontiers of robotic endoscopic capsules: a review. *Journal of micro-bio robotics*, 11(1):1–18, 2016.

[20] Margaret M Coad, Laura H Blumenschein, Sadie Cutler, Javier A Reyna Zepeda, Nicholas D Naclerio, Haitham El-Hussieny, Usman Mehmood, Jee-Hwan Ryu, Elliot W Hawkes, and Allison M Okamura. Vine Robots. *IEEE Robotics & Automation Magazine*, 27(3):120–132, 9 2020.

[21] Brian A Curran. Origami. *Encyclopaedia of the History of Science, Technology, and Medicine in Non-Western Cultures*, pages 1797–1800, 2008.

[22] David Dureisseix. An overview of mechanisms and patterns with origami. *International Journal of Space Structures*, 27(1):1–14, 3 2012.

[23] Yomna Elghazi, Ayman Wagdy, Sahar Abdelwahab, and Asmaa Hassan. Daylighting Driven Design: Optimizing Kaleidocycle façade for hot arid climate. 11 2014.

[24] Hongbin Fang, Yetong Zhang, and K W Wang. Origami-based earthworm-like locomotion robots. *Bioinspiration & Biomimetics*, 12(6):065003, 10 2017.

[25] J. M. Fitzpatrick and J. E.A. Wickham. Minimally invasive surgery. *The British journal of surgery*, 77(7):721–722, 1990.

[26] William E. Frazier. Metal additive manufacturing: A review. *Journal of Materials Engineering and Performance*, 23(6):1917–1928, 4 2014.

[27] Yukun Ge, Thilina Dulantha Lalitharatne, and Thrishantha Nanayakkara. Origami Inspired Design for Capsule Endoscope to Retrograde Using Intestinal Peristalsis. *IEEE Robotics and Automation Letters*, 7(2):5429–5435, 4 2022.

[28] Jonathan Golledge. Abdominal aortic aneurysm: update on pathogenesis and medical treatments. *Nature Reviews Cardiology 2018 16:4*, 16(4):225–242, 11 2018.

[29] Satyabodh Shesharaj Guttal, Ramesh K. Nadiger, and Pravinkumar Shetty. Cytotoxic effect of indigenously fabricated dental magnets for application in prosthodontics. *Journal of Indian Prosthodontist Society*, 18(1):29–34, 1 2018.

[30] Solomon Russom Habtay. A Firm-Level Analysis on the Relative Difference between Technology-Driven and Market-Driven Disruptive Business Model Innovations. *Creativity and Innovation Management*, 21(3):290–303, 9 2012.

[31] https://flowtoys.com/toroflux?srsltid=AfmBOopNcKq84draGfCjx5LjtTqwWbr-NU5NsemcauNxcQ1ba-FEYz6o and 28-11-2024. Toroflux.

[32] Jian Huang, Yongsheng Wang, Lin Lin, Zhibin Li, Zhonggui Shan, and Shaoyi Zheng. Comparison of dynamic changes in aortic diameter during the cardiac cycle measured by computed tomography angiography and transthoracic echocardiography. *Journal of Vascular Surgery*, 69(5):1538–1544, 5 2019.

[33] B. Jaffray. Minimally invasive surgery. *Archives of disease in childhood*, 90(5):537–542, 5 2005.

[34] Jaisohn Kim VT. Coding the Mass-Spring-Damper System in MATLAB (2/2).

[35] Semi Jeong, Hyunchul Choi, Gwangjun Go, Cheong Lee, Kyung Seob Lim, Doo Sun Sim, Myung Ho Jeong, Seong Young Ko, Jong Oh Park, and Sukho Park. Penetration of an artificial arterial thromboembolism in a live animal using an intravascular therapeutic microrobot system. *Medical Engineering & Physics*, 38(4):403–410, 4 2016.

[36] K.Wayne Johnston, Robert B. Rutherford, M.David Tilson, Dhiraj M. Shah, Larry Hollier, and James C. Stanley. Suggested standards for reporting on arterial aneurysms. *Journal of Vascular Surgery*, 13(3):452–458, 3 1991.

[37] Corinne Kruger and Nigel Cross. Solution driven versus problem driven design: strategies and outcomes. *Design Studies*, 27(5):527–548, 9 2006.

[38] Mohit Kshirsagar, Siddhi D. Ambike, Niranjana Jaya Prakash, Balasubramanian Kandasubramanian, and Pradnya Deshpande. Origami engineering: Creating dynamic functional materials through folded structures. *Hybrid Advances*, 4:100092, 12 2023.

[39] Robert J. Lang, Nathan Brown, Brian Ignaut, Spencer Magleby, and Larry Howell. Rigidly Foldable Thick Origami Using Designed-Offset Linkages. *Journal of Mechanisms and Robotics*, 12(2), 4 2020.

[40] Ruihua Li, Yang Liu, and Jianjun Jiang. Research advances in drug therapy for abdominal aortic aneurysms over the past five years: An updated narrative review. *International Journal of Cardiology*, 372:93–100, 2 2023.

[41] Patrick Z. McVeigh, Raphael Sacho, Robert A. Weersink, Vitor M. Pereira, Walter Kucharczyk, Eric J. Seibel, Brian C. Wilson, and Timo Krings. High-Resolution Angioscopic Imaging During Endovascular Neurosurgery. *Neurosurgery*, 75(2):171, 2014.

[42] Shuhei Miyashita, Steven Guitron, Kazuhiro Yoshida, Shuguang Li, Dana D. Damian, and Daniela Rus. Ingestible, controllable, and degradable origami robot for patching stomach wounds. In *2016 IEEE International Conference on Robotics and Automation (ICRA)*, pages 909–916. IEEE, 5 2016.

[43] Elissa Morris, Daniel A. McAdams, and Richard Malak. The State of the Art of Origami-Inspired Products: A Review. *Proceedings of the ASME Design Engineering Technical Conference*, 5B-2016, 12 2016.

[44] Kirsty Muldoon, Yanhua Song, Zeeshan Ahmad, Xing Chen, and Ming Wei Chang. High Precision 3D Printing for Micro to Nano Scale Biomedical and Electronic Devices. *Micromachines 2022, Vol. 13, Page 642*, 13(4):642, 4 2022.

[45] Ian M. Nordon, Robert J. Hinchliffe, Ian M. Loftus, and Matt M. Thompson. Pathophysiology and epidemiology of abdominal aortic aneurysms. *Nature Reviews Cardiology*, 8(2):92–102, 2 2011.

[46] Rui Peng and Gregory S. Chirikjian. A methodology for thick-panel origami pattern design. *Mechanism and Machine Theory*, 189:105423, 11 2023.

[47] Rui Peng and Gregory S. Chirikjian. Morphable thick-panel origami. *Mechanism and Machine Theory*, 192:105528, 2 2024.

[48] Nelson G Badillo Perez and Margaret M Coad. Self-Propelled Soft Everting Toroidal Robot for Navigation and Climbing in Confined Spaces. In *2022 IEEE/RSJ International Conference on Intelligent Robots and Systems (IROS)*, pages 5409–5415, 10 2022.

[49] Hossein Ramezani Ali-Akbari. Design-of-a-Satellite-Solar-Panel-Deployment-Mechanism-Using-the-Brushed-DC-Motor-as-Rotational-Speed-Damper. 1 2018.

[50] Gulnaaz Rasiya, Abhinav Shukla, and Karan Saran. Additive Manufacturing-A Review. *Materials Today: Proceedings*, 47:6896–6901, 1 2021.

[51] Kenny Seymour, Dakota Burrow, Alex Avila, Terri Bateman, David Morgan, Spencer Magleby, and Larry Howell. Origami-Based Deployable Ballistic Barrier. *Faculty Publications*, 9 2018.

[52] Metin Sitti, Hakan Ceylan, Wenqi Hu, Joshua Giltinan, Mehmet Turan, Sehyuk Yim, and Eric Diller. Biomedical Applications of Untethered Mobile Milli/Microrobots. *Proceedings of the IEEE*, 103(2):205–224, 2 2015.

[53] P.W. Stather, D.A. Sidloff, I.A. Rhema, E. Choke, M.J. Bown, and R.D. Sayers. A Review of Current Reporting of Abdominal Aortic Aneurysm Mortality and Prevalence in the Literature. *European Journal of Vascular and Endovascular Surgery*, 47(3):240–242, 3 2014.

[54] Stephan Haulon. Golden rules to perform complex EVAR in daily practice, 5 2017.

[55] Austin Taylor, Matthew Miller, Mable Fok, Kent Nilsson, and Zion Tsz Ho Tse. Intracardiac magnetic resonance imaging catheter with origami deployable mechanisms. *Journal of Medical Devices, Transactions of the ASME*, 10(2), 6 2016.

[56] Sam Tijhuis. *A Modeling Framework for Magnetic Origami Devices using a Bar-and-Hinge Model*. PhD thesis, 6 2024.

[57] G M Van Vliet. *DESIGN OF A COMPLIANT MAGNETIC CAPSULE ROBOT FOR UNTETHERED CARDIOVASCULAR SURGICAL TOOLS*. PhD thesis, 2021.

[58] Kaufui V. Wong and Aldo Hernandez. A Review of Additive Manufacturing. *International Scholarly Research Notices*, 2012(1):208760, 1 2012.

[59] Oncay Yasa, Yasunori Toshimitsu, Mike Y. Michelis, Lewis S. Jones, Miriam Filippi, Thomas Buchner, and Robert K. Katzschmann. An Overview of Soft Robotics. *Annual Review of Control, Robotics, and Autonomous Systems*, 6(Volume 6, 2023):1–29, 5 2023.

[60] Hiromi Yasuda, Yasuhiro Miyazawa, Efstathios G. Charalampidis, Christopher Chong, Panayotis G. Kevrekidis, and Jinkyu Yang. Origami-based impact mitigation via rarefaction solitary wave creation. *Science Advances*, 5(5), 2019.

[61] Sishen Yuan, Sifan Cao, Junnan Xue, Shijian Su, Junyan Yan, Min Wang, Wenchao Yue, Shing Shin Cheng, Jun Liu, Jiaole Wang, Shuang Song, Max Q.H. Meng, and Hongliang Ren. Versatile Motion Generation of Magnetic Origami Spring Robots in the Uniform Magnetic Field. *IEEE Robotics and Automation Letters*, 7(4):10486–10493, 10 2022.

[62] Abolfazl Zolfaghari, Tiantong Chen, and Allen Y. Yi. Additive manufacturing of precision optics at micro and nanoscale. *International Journal of Extreme Manufacturing*, 1(1):012005, 4 2019.

9 Appendex

9.1 Morphological diagram

Key features	Options
Locomotion	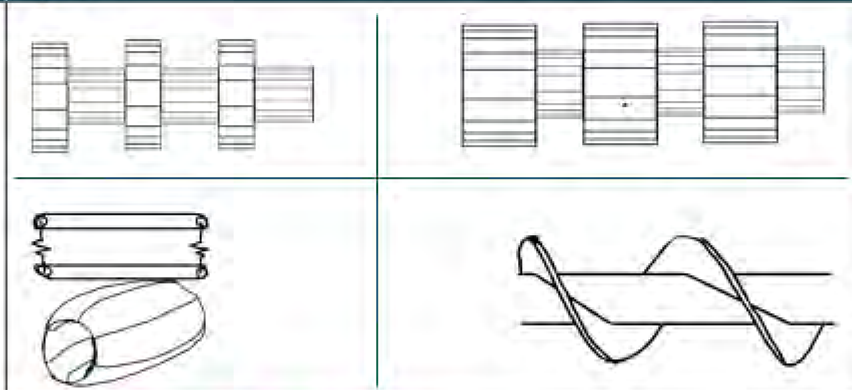
Aortic adaptability	
Base shape	
Modulation method	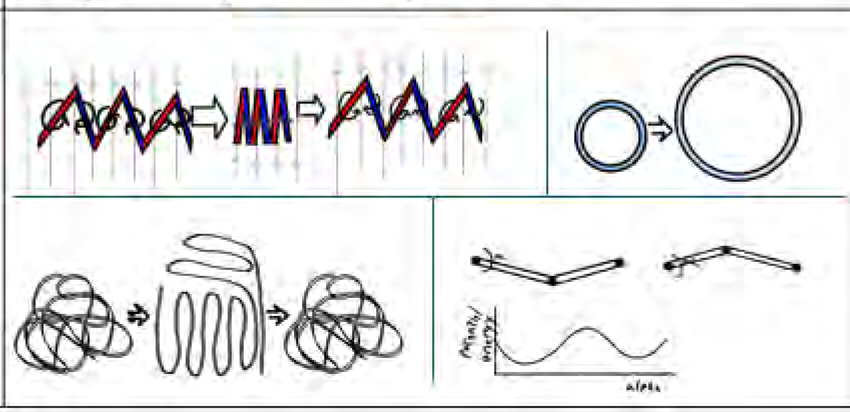

9.2 Lasercutter setup

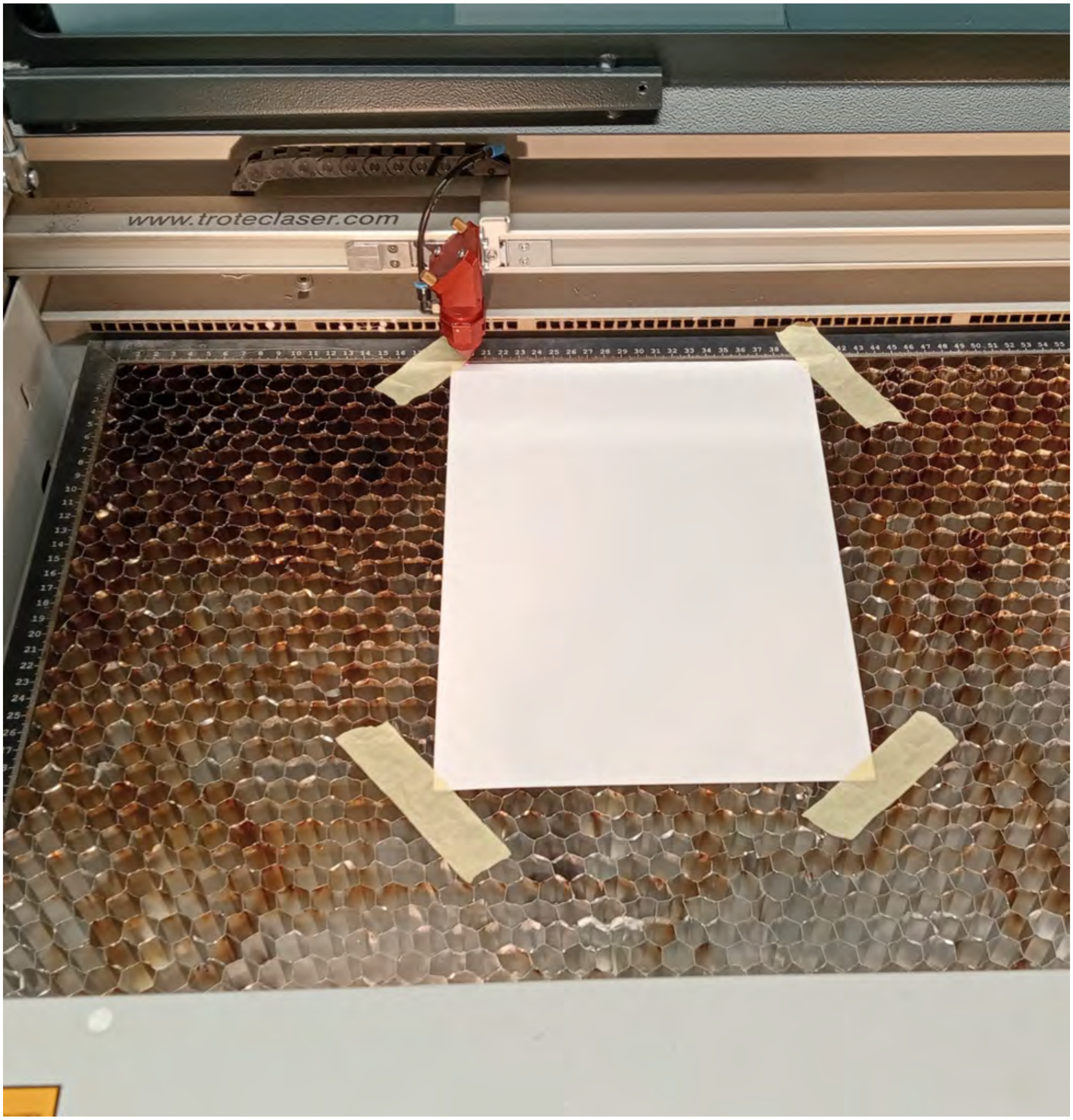

9.3 Lasercutter results

9.3.1 Results 50g paper

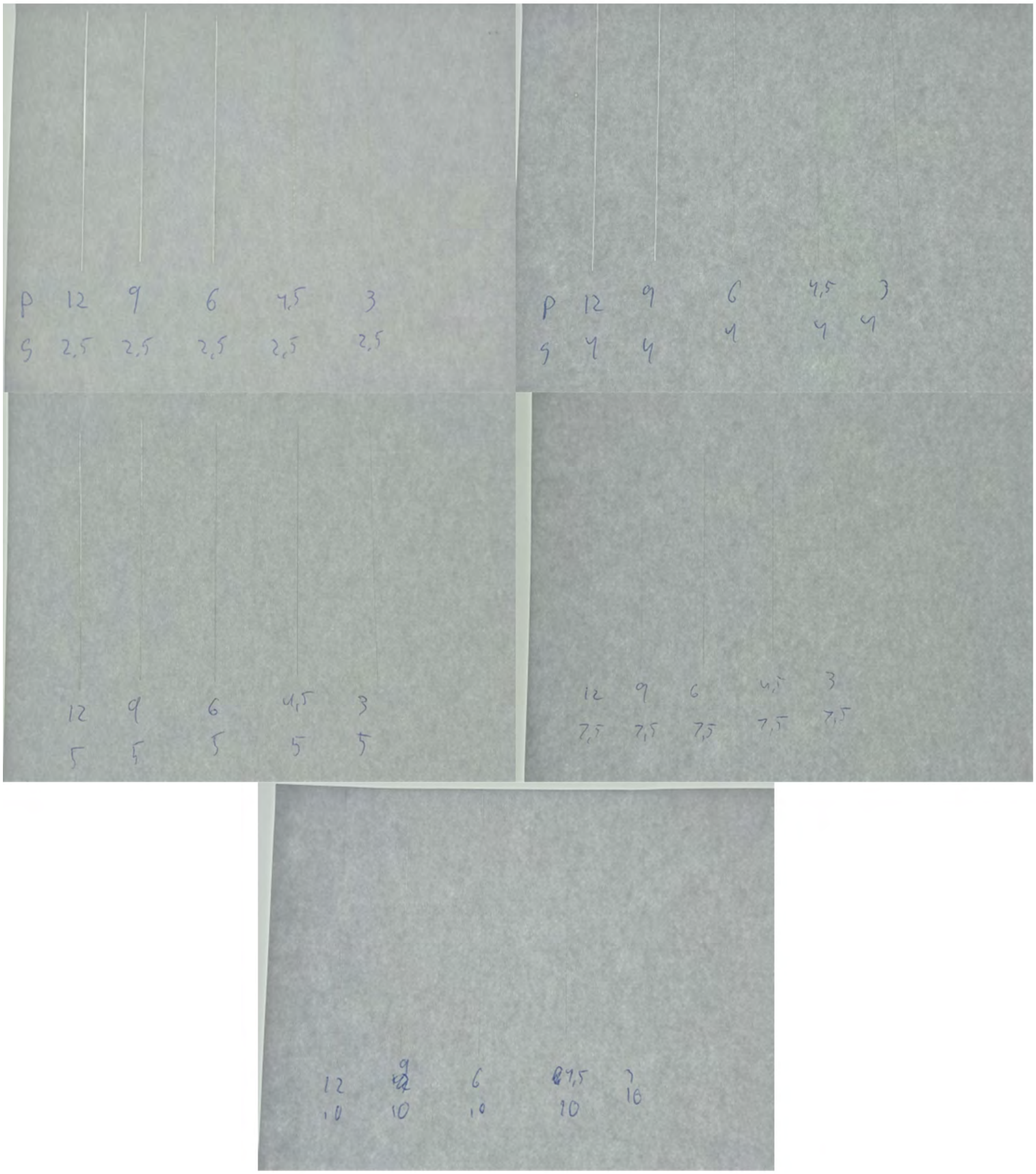

9.3.2 Results 80g paper

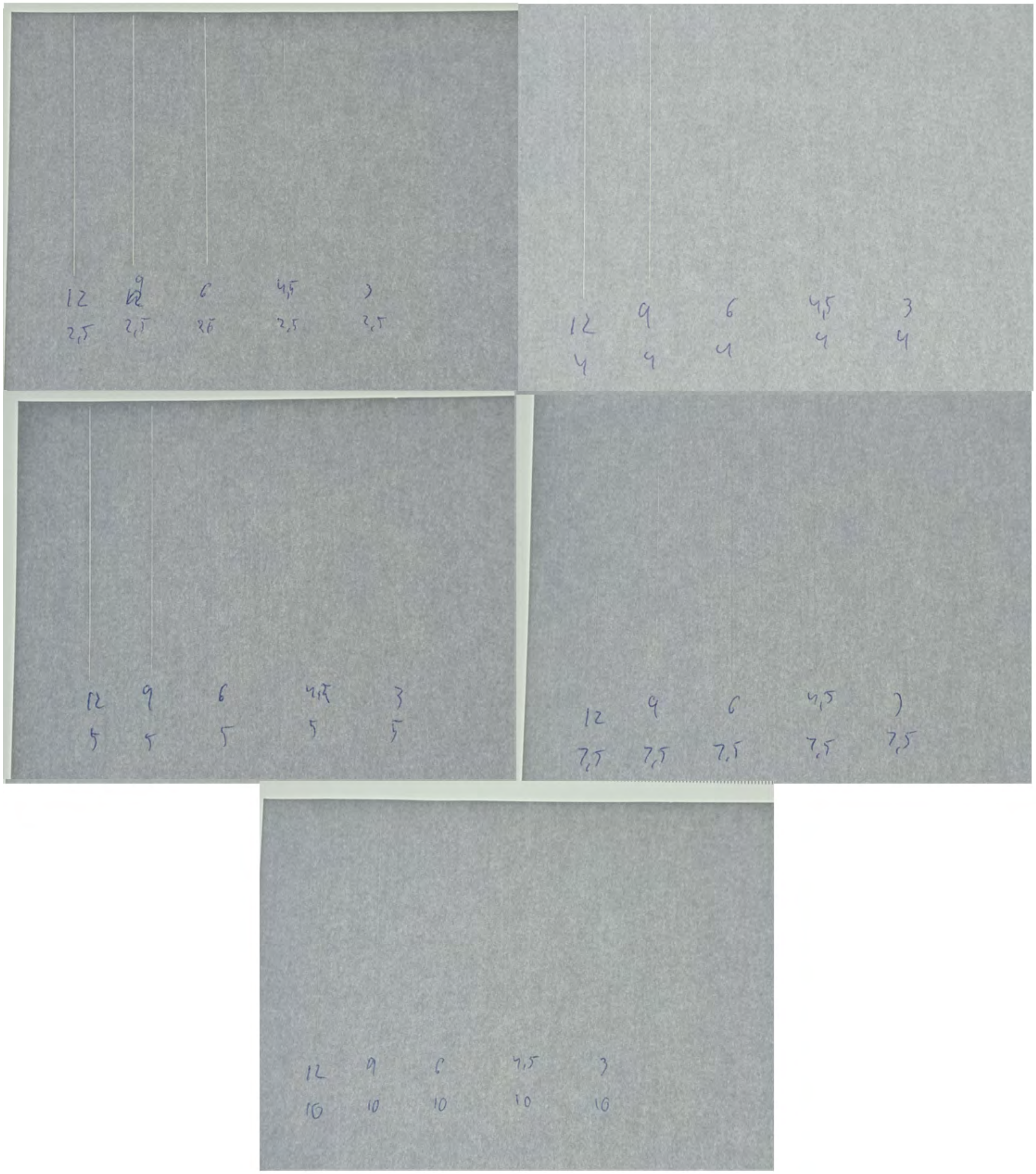

9.3.3 Result table

Table 8: Results 50 gsm paper. C=cut, C/G=Almost good engraving but parts are cut, G=good engraving, G/N=There is engraving but it is very shallow, N=no engraving, P=perforation

power%\speed	**2.5**	**4**	**5**	**7.5**	**10**
3	**G/N**	**N**	**N**	**N**	**N**
4.5	**C/G**	**G**	**N**	**N**	**N**
6	**C**	**C/G**	**G**	**G/N**	**N**
9	**C**	**C**	**C/G**	**G**	**P**
12	**C**	**C**	**C**	**C/G**	**P**

Table 9: Results 80 gsm paper. C=cut, C/G=Almost good engraving but parts are cut, G=good engraving, G/N=There is engraving but it is very shallow, N=no engraving, P=perforation

power%\speed	**2.5**	**4**	**5**	**7.5**	**10**
3	**G/N**	**N**	**N**	**N**	**N**
4.5	**C/G**	**G/N**	**N**	**N**	**N**
6	**C**	**G**	**G**	**N**	**N**
9	**C**	**C/G**	**P**	**P**	**P**
12	**C**	**C**	**C**	**G**	**G**